J. Plasma Physics (2004), *vol.* 70, *part* 5, *pp.* 505–532.
DOI: 10.1017/S0022377803002745 Printed in the United Kingdom

Transport of energetic charged particles. Part 2. Small-angle scattering

E. Kh. KAGHASHVILI,[1] G. P. ZANK,[1]
J. Y. LU[2,4] and W. DRÖGE[3,5]

[1]Institute of Geophysics and Planetary Physics and Department of Physics, University of California, Riverside, CA 92521, USA
(zank@ucrac1.ucr.edu)

[2]Department of Physics, University of Alberta, Edmonton, Alberta, Canada T6G 2J1

[3]Bartol Research Institute, University of Delaware, Newark, DE 19716, USA

[4]Center for Space Science and Applied Research, Chinese Academy of Sciences, Beijing, 100080, China

[5]Institut fur Experimentelle und Angewandte Physik, Universitat Kiel, D-24118 Kiel, Germany

(Received 1 October 2003)

Abstract. The propagating source method has been extended to solve the Boltzmann equation with a quasi-linear diffusion scattering operator. A half-range polynomial expansion method is used to reduce the integral-diffusion form of the 'collisional' Boltzmann equation to an infinite set of linear hyperbolic partial differential equations in the harmonics of the polynomial expansion. The lowest-order truncation of the coupled set of equations yields an inhomogeneous form of the well-known telegrapher equation, which, unlike the homogeneous telegrapher equation, does not introduce physically unrealistic pulse solutions. Anisotropic quasi-linear scattering models for which the index q of the power spectrum of magnetic fluctuations satisfies $1 < q < 2$ admit slow scattering through 90° and no scattering through 90° for $q \geqslant 2$. Accordingly, four models that either allow or enhance scattering through 90° are used to augment the standard quasi-linear model for pitch-angle scattering. These are mirroring, dynamical turbulence and two distinct wave-based models. In the case that mirroring is responsible for scattering particles through 90°, together with the standard QLT (quasi-linear theory) pitch-angle diffusion model for scattering within the forward and backward hemispheres, it is found that the QLT isotropic and anisotropic models are well approximated by relaxation time scattering models. As an application of the general study, the implications of the four models introduced to redress the difficulties faced by QLT in describing scattering through 90° are briefly considered. An initial beam was found to relax more rapidly for either the dynamical turbulence or wave models with resonant scattering through 90° than for mirroring models.

1. Introduction

The transport of charged particles along a randomly fluctuating magnetic field is a basic problem in space physics and astrophysics. Typically, the magnetic field is ordered on some large scale but is highly temporal on smaller scales. In Part 1 of

this series of papers (Zank et al. 1999, 2000; henceforth Paper 1), we introduced a new approach, the propagating source method, for solving the time-dependent Boltzmann equation for charged particles experiencing large-angle deflections ('collisions') in the fluctuating magnetic field. In Paper 1, the large-angle scattering operator was modeled as a BGK (Bhatnager, Gross and Krook 1954) relaxation time operator. In this paper, we extend the propagating source method to a small-angle quasi-linear scattering operator that takes the form of a diffusion term in the cosine of particle pitch-angle. In addition to describing the general method and presenting some results, we apply this approach to the general question of particle scattering through 90° and present a brief comparison of large-angle and small-angle scattering models. The transport of charged particles along a magnetic field is governed by the Fokker–Planck equation. By assuming that the charged particle distribution function $f(\mathbf{x}, t, \mathbf{v})$ is nearly gyrotropic, the gyrophase averaged Boltzmann equation in the stationary frame may be expressed as (Skilling 1971; Isenberg 1997)

$$\frac{\partial f}{\partial t} + (u_i + v\mu b_i)\frac{\partial f}{\partial x_i} + \left[\frac{1-3\mu^3}{2} b_i b_j \frac{\partial u_i}{\partial x_j} - \frac{1-\mu^3}{2}\frac{\partial u_i}{\partial x_i} - \frac{\mu b_i}{v}\left(\frac{\partial u_i}{\partial t} + u_j \frac{\partial u_i}{\partial x_j}\right)\right] v\frac{\partial f}{\partial v} + \frac{1-\nu^2}{2}\left[v\frac{\partial b_i}{\partial x_i} + \mu\frac{\partial u_i}{\partial x_i} - 3\mu b_i b_j \frac{\partial u_i}{\partial x_j} - \frac{2b_i}{v}\left(\frac{\partial u_i}{\partial t} + u_j\frac{\partial u_i}{\partial x_j}\right)\right]\frac{\partial f}{\partial \mu} = \left(\frac{\delta f}{\delta t}\right)_c + S - L. \tag{1.1}$$

In (1.1), the distribution function $f(\mathbf{x}, t, \mathbf{v}) = f(\mathbf{x}, t, \mu, v)$, where the pitch angle θ defines $\mu \equiv \mathbf{v}\cdot\mathbf{b}/\mathbf{v} = \cos\theta$, $\mathbf{b} = \mathbf{B}_0/|\mathbf{B}_0|$ is the unit vector aligned with the large-scale magnetic field $\mathbf{B}_0$, v denotes the particle speed along $\mathbf{B}_0$ and $\mathbf{u}$ is the large-scale bulk flow velocity. The variables $\mathbf{x}$ and t denote the particle position and time respectively and S and L are source and loss terms, respectively. Cross-field diffusion and particle drifts are neglected in (1.1), as is energy diffusion. For the present, we restrict our attention to large particle energies (i.e. $v \gg u$) and consider a constant flow speed u and radial magnetic field. We further neglect focusing and adiabatic deceleration. Subject to these assumptions, the equation that we solve is therefore

$$\frac{\partial f}{\partial t} + \mu v \frac{\partial f}{\partial x_i} = \left(\frac{\delta f}{\delta t}\right)_c. \tag{1.2}$$

This very simplified form of the Boltzmann equation is often used to study cosmic-ray propagation in the heliosphere (e.g. Kota 1994).

2. Models for $D_{\mu\mu}$ and scattering through 90°

The scattering operator $(\delta f/\delta t)_c$ in (1.2) describes particle scattering by random magnetic fluctuations and is given either by a quasi-linear pitch-angle model or by a relaxation time model. Paper 1 considered large-angle scattering, using a relaxation time model, exclusively. We extend the approach of Paper 1 to include the small-angle quasi-linear scattering operator.

https://doi.org/10.1017/S0022377803002745 Published online by Cambridge University Press

For pitch-angle scattering, the scattering operator is frequently expressed in terms of particle diffusion in the pitch angle. Thus,

$$\left(\frac{\delta f}{\delta t}\right)_c = \frac{\partial}{\partial \mu}\left[D_{\mu\mu}(\mu,\tau_1)\frac{\partial f}{\partial \mu}\right], \tag{2.1}$$

where $D_{\mu\mu}(\mu,\tau_1)$ is the particle scattering frequency (e.g. Jokipii 1966) and is a function of the pitch-angle and the quasi-linear small-angle scattering time τ_1. If the magnetic field fluctuations are assumed to be magnetostatic, the turbulence geometry is assumed to be slab and the spectral form is proportional to k^{-q} (where k denotes wave number), then $D_{\mu\mu}(\mu,\tau_1)$ may be expressed in the form (Jokipii 1966; Hasselmann and Wibberanz 1968)

$$D^{\mathrm{QLT}}_{\mu\mu}(\mu,\tau_1) = \frac{|\mu|^{q-1}(1-\mu^2)}{\tau_1}. \tag{2.2}$$

The time scale τ_1 is determined from a combination of the particle frequency Ω, the mean magnetic field strength B_0 and the particle velocity v (e.g. Dröge 2000b). Specifically, if we assume that the power spectrum of resonant scattering waves or turbulence has the form $P = Ak^{-q}$ for wavenumber k, then

$$\tau_1^{-1} \equiv \frac{\pi}{4}\frac{A\Omega^{2-q}v^{q-1}}{B_0^2}.$$

The BGK Boltzmann collision operator or relaxation time approximation

$$\left(\frac{\delta f}{\delta t}\right)_c = \frac{\langle f\rangle - f}{\tau} \tag{2.3}$$

is often used instead of (2.1) (Gombosi et al. 1993; Kota 1994; Zank et al. 2000; Lu and Zank 2001; Lu et al. 2001) and describes isotropic large-angle scattering. In (2.3), $\langle f\rangle \equiv \frac{1}{2}\int_{-1}^{1} f\,d\mu$ is the isotropic distribution function f averaged over the pitch angle μ and $\tau = \tau(\mathbf{x}, v, \mu)$ is a collision or scattering time.

The scattering of particles through $\mu = 0$ has long been regarded as a major challenge to models of particle transport, particularly those based on a QLT diffusion formulation such as (2.2). Evidently, a magnetic fluctuation spectrum for which the spectral index satisfies $q = 1$ corresponds to isotropic scattering and particles experience no difficulty at 90°. However, for $q > 1$, the scattering time tends to infinity as $|\mu| \to 0$. Since the parallel mean free path $\lambda_\parallel$ is given by

$$\lambda_\parallel \propto \int_{-1}^{1} \frac{(1-\mu^2)^2}{D_{\mu\mu}}\,d\mu,$$

use of (2.2) shows that $\lambda_\parallel^{-1}$ remains bounded provided $q < 2$. For $q \geqslant 2$, the integral for $\lambda_\parallel$ is divergent. What this implies, of course, is that the flux of particles in momentum space through $\mu = 0$ is non-zero provided that $1 < q < 2$. Physically, the non-zero flux through $\mu = 0$ has the following interpretation. For a particle located at $\epsilon > 0$ say in velocity space, the location being determined precisely by the resonance condition, a scatter will change ϵ to $\epsilon + \Delta\mu = \epsilon'$. For ϵ small, i.e. close to $\mu = 0$, the $\Delta\mu$ change can be sufficiently large so that the particle scatters through 90° and $\epsilon' < 0$. Provided the turbulence spectrum is sufficiently flat, such $\Delta\mu$ scatters ensure a non-zero flux in momentum space through 90°. Conversely, if the spectrum is too steep and $\Delta\mu$ is very small due to insufficient power near 90°, then a particle can never be 'close enough' to $\mu = 0$ for it to scatter through 90°.

https://doi.org/10.1017/S0022377803002745 Published online by Cambridge University Press

Thus, for $q \neq 1$, particles cannot scatter *from* 90°, and for $1 < q < 2$, particles can scatter *through* 90°. Thus, since the dissipation range of the magnetic fluctuation spectrum typically satisfies $q > 2$ (where particles with very small pitch angles are expected to resonate), it has been argued by Davila and Scott (1984); (see also Bieber et al. (1988); Smith et al. (1990)) that scattering through 90° is prevented by the dissipation of turbulence at the small scales. As a result, the mean free path in standard QLT is formally infinite.

In an effort to address the shortcomings of standard QLT with respect to scattering through 90°, several mechanisms have been suggested which either augment or refine the diffusion theory. Among these are 'mirroring' by fluctuations of the magnetic field magnitude (Goldstein et al. 1974; Smith 1992), nonlinear extensions of QLT (Goldstein 1976; Jones et al. 1978; Owens 1974; Völk 1975), resonance broadening (Völk 1973; Dröge 1994), wave propagation effects (Schlickeiser 1988, 1989; Schlickeiser et al. 1991; Dröge and Schlickeiser 1993; Schlickeiser and Achatz 1993; Dröge 2000a, b), dynamical turbulence (Bieber and Matthaeus 1991, 1992; Bieber et al. 1994) and non-resonant pitch-angle scattering (Ragot 1999, 2000). A review of models describing the various approaches to the scattering of particles through 90° is given by Dröge (2000b).

The relaxation time scattering operator (2.3) can be extended to accommodate the possibility of non-isotropic particle scattering when particles have difficulty in scattering through 90°. One way is to introduce two scattering time scales τ_1 and τ_2. In the $\mu < 0$ and $\mu > 0$ hemispheres of velocity space, particle scattering is assumed to be isotropic and to occur at a rate τ_1^{-1}. By contrast, the scattering of particles from one hemisphere to another proceeds at the slower rate τ_2^{-1}. Thus, $\mu = 0$ is singular in the sense that scattering through 90° is slow. Following Kota (1994), Zank et al. (2000) adopted a modified relaxation time model analogous to (2.3) and introduced the half-range expansion $f^{\pm}$ corresponding to particles populating either the forward ($\mu > 0$) or backward ($\mu < 0$) hemispheres. Schwadron (1998) introduced a similar scattering operator in his modeling of solar wind pickup ion propagation (see also Isenberg (1997)). Accordingly, we may generalize (1.2) as

$$\frac{\partial f^-}{\partial t} + \mu v \frac{\partial f^-}{\partial r} = \frac{\langle f^- \rangle - f^-}{\tau_1} + \frac{\langle f^+ \rangle - f^-}{\tau_2}, \quad (\mu < 0) \tag{2.4}$$

$$\frac{\partial f^+}{\partial t} + \mu v \frac{\partial f^+}{\partial r} = \frac{\langle f^+ \rangle - f^+}{\tau_1} + \frac{\langle f^- \rangle - f^+}{\tau_2}, \quad (\mu > 0) \tag{2.5}$$

where $\langle f^- \rangle \equiv \frac{1}{2}\int_{-1}^{0} f^- \, d\mu$ and $\langle f^+ \rangle \equiv \frac{1}{2}\int_{0}^{1} f^+ \, d\mu$. If $\tau_1 = \tau_2 = 2\tau$, then the isotropic scattering model (1.2) is recovered.

In this paper, we assume simple functional forms for the scattering operators appropriate to some of the above models advanced to resolve the 90° QLT scattering problem and compare the resulting solutions for identical initial data. As we show, some of the theoretical models advanced to scatter particles through 90° lead to observable differences in the computed distribution functions. Elsewhere (Lu et al. 2002), we use a more realistic Boltzmann equation model that includes a background flow field, focusing and adiabatic deceleration for a particular model to study transport in the solar wind.

The scattering models are listed in Table 1. Four models are considered for the scattering of particles through 90°.

https://doi.org/10.1017/S0022377803002745 Published online by Cambridge University Press

Table 1. Four mechanisms considered for scattering particles through 90°. Also listed are the specific forms of either the collisional term or the Fokker–Plank coefficient $D_{\mu\mu}$ used to model scattering (including 90°) in this paper.

Mechanisms for scattering through 90°	Model scattering coefficients
(1) Mirroring	$\left(\frac{\delta f}{\delta t}\right)_c \approx \frac{\partial}{\partial \mu}\left(D_{\mu\mu}^{\mathrm{QLT}}\frac{\partial f}{\partial \mu}\right) + \frac{\langle f\rangle - f}{\tau_2}$
(2) Dynamical turbulence	$D_{\mu\mu} \approx D_{\mu\mu}^{\mathrm{QLT}} + \Phi(\mu=0)(1-\mu^2)$
(3) Wave models (resonant scattering)	$D_{\mu\mu} \approx D_{\mu\mu}^{\mathrm{QLT}} + \varphi\frac{1-\mu^2}{\tau_{\mathrm{res}}}$
(4) Wave models (non-resonant scattering)	$D_{\mu\mu} \approx D_{\mu\mu}^{\mathrm{QLT}} + \varphi^2\frac{1-\mu^2}{2\tau_{\mathrm{res}}}$
	$\varphi \equiv V_{\mathrm{group}}/v \approx V_{\mathrm{A}}/v$

(1) Mirroring or large-angle scattering of particles through 90°, which is assumed to proceed at a rate significantly slower than the pitch-angle scattering of particles, taken to occur independently within the forward and backward hemispheres. The pitch-angle scattering is described by the standard QLT Fokker–Planck diffusion coefficient (2.2).

(2) Model 2 is a slight generalization of one suggested by Bieber et al. (1994). By no longer assuming the usual magnetostatic approximation and introducing a decorrelation time for the magnetic turbulence, Bieber and Matthaeus (1991) introduced resonance broadening to allow particles to scatter through 90°. The decorrelation or two-point correlation decay time was estimated to be $(kV_{\mathrm{A}})^{-1}$ for a wave number k and Alfvén speed V_{A}. For protons, Bieber et al. (1994) found that the Fokker–Planck coefficient for pitch-angle scattering in dynamical turbulence was non-zero at 90°, and that it could be approximated by $\Phi(0)(1-\mu^2)$, where $\Phi(0) = (2\pi\Omega^2/B_0^2)G_{\mathrm{E}}(\Omega)$. Here, $G_{\mathrm{E}}(\Omega)$ denotes the Eulerian frequency spectrum ((3) of Bieber et al. (1994)). As can be seen from Fig. 7(b) of Bieber et al. (1994), the simple extension listed in Table 1 captures the features of the Fokker–Planck coefficient as a function of the pitch-angle.

(3) In a formal sense, the resonance broadening models introduced by Bieber and Matthaeus (1991) and Bieber et al. (1994) are related closely to the wave models introduced by Schlickeiser (1988, 1989) (see also Schlickeiser et al. (1991); Dröge and Schlickeiser (1993); Schlickeiser and Achatz (1993); Dröge 2000a, b). The wave models incorporate the dynamical effects of wave propagation, particularly waves propagating parallel and anti-parallel to the magnetic field, and damping in the scattering coefficient. The spectral functions adopted to describe the waves are not unlike the slab turbulence models introduced by Bieber et al. (1994) and, consequently, the wave and turbulence models can be described using the same mathematical formalism but with a different choice of parameter. At the simplest level of description, we therefore use the form listed in Table 1.

(4) Unlike the turbulence and wave models discussed above, Ragot (1999, 2000) has suggested that fast non-resonant magnetosonic waves can scatter low-rigidity cosmic rays through 90° very efficiently. Her argument is that low-frequency waves determine the local variation in the magnetic field line direction and

any description of particle scattering through $\mu = 0$ must therefore include the non-resonant low-frequency wave component. An approximate non-resonant diffusion coefficient $D_{\mu\mu} = \epsilon^2/(2\tau_{\rm exit})$ can be derived, where $\epsilon = V_{\rm A}/v$ is the ratio of the wave group velocity $V_{\rm group} \approx V_{\rm A}$ to the particle velocity. The average exit time $\tau_{\rm exit}$ describes the time for a particle to escape from a small μ neighborhood into a region where scattering can proceed more quickly by regular QLT diffusion in pitch angle. As suggested by Ragot (1999), the exit time is always less than the gyroperiod Ω^{-1}. Accordingly, we introduce the simple functional form shown in Table 1, which is a sum of the standard QLT diffusion coefficient for pitch angles not in the region $\mu \approx 0$ and the Ragot non-resonant term for $\mu \approx 0$.

3. Basic method

To illustrate our approach to solving the Boltzmann equation (1.2), we use the expressions for $D_{\mu\mu}$ listed in Table 1. We consider three distinct cases for the spectral wave number exponent: $q = 1$, which yields isotropic scattering; $q = 2$, which corresponds to pickup ion driven turbulence (Galeev and Sagdeev 1988; Glassmeier et al. 1989; Williams and Zank 1994); and $q = \frac{5}{3}$, which corresponds to the Kolmogorov spectrum typical of much of the solar wind (e.g. Matthaeus et al. 1995).

3.1. Case $q = 1$

As noted, the pitch-angle diffusion coefficient for this case admits only isotropic scattering with no singularity at 90°. Thus, in the absence of both focusing and adiabatic energy changes, the Boltzmann equation reduces to

$$\frac{\partial f}{\partial t} + \mu v \frac{\partial f}{\partial r} = \frac{\partial}{\partial \mu}\left(\frac{1-\mu^2}{\tau}\frac{\partial f}{\partial \mu}\right), \tag{3.1}$$

where $f(r, t, \mu, v)$ is the velocity space distribution function at position r and time t for particles of speed v and pitch angle cosine $\mu = \cos\theta$. We consider the Cauchy problem for (3.1) with arbitrary initial data given by

$$f(r, t = 0, \mu, v) = F(r, 0, \mu, v). \tag{3.2}$$

No restrictions are imposed on the form of the initial data, i.e. it need not be isotropic and we shall frequently consider an initial ring-beam distribution for which

$$F(r, 0, \mu, v) = \frac{N(r)\delta(v - v_0)\delta(\mu - \mu_0)}{2\pi v^2}. \tag{3.3}$$

In (3.3), $N(r)$ denotes the particle number density as a function of position.

As discussed in Paper 1 (see also Gombosi et al. (1993); Lu et al. (2001)) in the context of large-angle scattering, at very early times an initial particle distribution should propagate almost ballistically until such time as scattering begins to modify the distribution. Thus, particle scattering may be viewed as a loss process for the unscattered streaming particles with a decay time given by the scattering time τ. Conversely, no scattered particles exist at early times and instead the scattered distribution grows from zero as the unscattered streaming distribution decays. Thus, initial data can be prescribed for the unscattered particle distribution, which, as it decays, leads to the formation of a scattered particle distribution.

https://doi.org/10.1017/S0022377803002745 Published online by Cambridge University Press

This approach was discussed originally by Zank et al. (1999) and is reminiscent of the multiple scattering solution of the Boltzmann equation presented by Webb et al. (1999, 2000). Since we are at liberty to separate the distribution function in any way we choose, provided that we ensure that the appropriate initial and boundary conditions between f^{s} and F hold, the above comments suggest we split the distribution function f into an 'unscattered' part F and a 'scattered' part f^{s} according to the decomposition

$$f = f^{\mathrm{s}} + F \tag{3.4}$$

and (3.1) may be re-expressed as

$$\frac{\partial F}{\partial t} + \mu v \frac{\partial F}{\partial r} = -\frac{F}{\tau}, \tag{3.5}$$

$$\frac{\partial f^{\mathrm{s}}}{\partial t} + \mu v \frac{\partial f^{\mathrm{s}}}{\partial r} = \frac{\partial}{\partial \mu}\left(\frac{1-\mu^2}{\tau}\frac{\partial f^{\mathrm{s}}}{\partial \mu}\right) + \frac{\partial}{\partial \mu}\left(\frac{1-\mu^2}{\tau}\frac{\partial F}{\partial \mu}\right) + \frac{F}{\tau}. \tag{3.6}$$

We can verify *a posteriori* that the decomposition of (3.1) into (3.5) and (3.6) is valid since the solution F of (3.5) with the initial data (3.2) is the ballistically propagating, decaying distribution

$$F(r,t,\mu,v) = F(r-\mu v t, 0, \mu, v)e^{-t/\tau}. \tag{3.7}$$

Note that F can only lose particles unless an explicit source term is present (such as occurs for pickup ions in the inner and outer heliosphere). Evidently, F is a source term for the scattered particle distribution and, unlike the prescribed initial data, is a moving source. As discussed in Paper 1, such a distributed source of scattered particles acts to eliminate the possibility of coherent pulses forming for isotropic scattering when a low-order truncation to a polynomial series solution to (3.1) is used.

To solve (3.6), we may expand f^{s} in an infinite series of Legendre polynomials $P_n(\mu)$,

$$f^{\mathrm{s}}(r,t,\mu,v) = \sum_{n=0}^{\infty}(2n+1)P_n(\mu)f_n(r,t,v), \tag{3.8}$$

where $f_n(r,t,v)$ is the nth harmonic of the scattered distribution function

$$f_n(r,t,v) = \frac{1}{2}\int_{-1}^{1} P(\mu)f^{\mathrm{s}}(r,t,\mu,v)\,d\mu. \tag{3.9}$$

By means of the recursion relations $(n+1)P_{n+1}(\mu) + nP_{n-1}(\mu) = (2n+1)\mu P_n(\mu)$ and $(\mu^2-1)P_n'(\mu) = n\mu P_n(\mu) - nP_{n-1}(\mu)$ (the prime denotes differentiation), we obtain the infinite set of partial differential equations for the harmonics of the scattered distribution f^{s}

$$\frac{\partial f_n}{\partial t} + \frac{(n+1)v}{2n+1}\frac{\partial f_{n+1}}{\partial r} + \frac{nv}{2n+1}\frac{\partial f_{n-1}}{\partial r} = -(n^2+n-1)\frac{F_n}{\tau} - n(n+1)\frac{f_n}{\tau}. \tag{3.10}$$

https://doi.org/10.1017/S0022377803002745 Published online by Cambridge University Press

The source term F_n in (3.10) is of course the nth harmonic of the decaying unscattered distribution F. The formal structure of the partial differential equations (3.10) is very similar to those derived for the large-angle scattering case discussed in Paper 1, with a primary difference being the presence of the higher-order harmonic source terms.

The closure of (3.10) is commonly addressed by simply truncating the infinite set of equations at some arbitrary order with the hope that this does not introduce any unphysical character into the reduced model. For the f_1 approximation (i.e. assume $f_n = 0$, for all $n \geqslant 2$), we have

$$\begin{aligned} \frac{\partial f_0}{\partial t} + v\frac{\partial f_1}{\partial r} &= \frac{F_0}{\tau}, \\ \frac{\partial f_1}{\partial t} + \frac{v}{3}\frac{\partial f_0}{\partial r} &= -\frac{F_1}{\tau} - \frac{2f_1}{\tau}, \end{aligned} \tag{3.11}$$

which is a linear hyperbolic system admitting the characteristic speeds $\lambda = \pm v/\sqrt{3}$, a result which is entirely independent of the form of the scattering operator. Equations (3.11) can be combined to give the more familiar telegrapher equation, although now in inhomogeneous form because of the source terms F_0 and F_1,

$$\tau\frac{\partial^2 f_0}{\partial t^2} + 2\frac{\partial f_0}{\partial t} - \kappa\frac{\partial^2 f_0}{\partial r^2} = \frac{\partial F_0}{\partial t} + v\frac{\partial F_1}{\partial r} + \frac{2F_0}{\tau} \tag{3.12}$$

and $\kappa \equiv v^2\tau/3 = (4/3\pi)v^2B_0^2/(\Omega A)$. The inhomogeneous term in (3.12) is the source term for the isotropic scattered component and the initial data is only with respect to F in (3.7). As in Paper 1, the inhomogeneous telegrapher equation can be solved analytically, yielding a somewhat cumbersome expression. The exact solution of (3.12) reveals several important features which distinguish the transport equation (3.12) from the standard telegrapher equation model. The scattered particle distribution grows gradually from zero at the initial time. The combined distribution $f = F + (f_0 + 3\mu f_1)$ describes the evolution of the particle distribution function at all times, including $t < \tau$. The expansion which yields the linear hyperbolic equations (3.12) (and the higher order expansion (3.13) below) captures the initial coherent or flash phase (Earl 1995; Federov and Shakhov 1993; Federov et al. 1995; Ruffulo and Khumlumlert 1995) of particle transport together with the subsequent evolution into the diffusive regime. Furthermore, no coherent pulses are present in the solution of (3.12) and this, as discussed in Paper 1, is a consequence of the propagating source term. The inhomogeneous telegrapher equation is therefore a major improvement in describing particle propagation compared with the original telegrapher equation formulated by Fisk and Axford (1969).

In general, the f_n truncation forms a linear hyperbolic system of partial differential equations

$$\Psi_t + v\mathscr{A}\Psi_r = \mathscr{C} \tag{3.13}$$

with a (discrete) spectrum of characteristic speeds. Here $\Psi = (f_0, f_1, f_2, \ldots c)^{\mathrm{T}}$, with T denoting transpose, the subscripts denoting partial differentiation with respect

https://doi.org/10.1017/S0022377803002745 Published online by Cambridge University Press

to t and r, and $\mathscr{A}$ is the tridiagonal matrix

$$\mathscr{A} = \begin{pmatrix} 0 & 1 & 0 & 0 & 0 & \dots & \dots & 0 \\ \frac{1}{3} & 0 & \frac{2}{3} & 0 & 0 & \dots & \dots & 0 \\ 0 & \frac{2}{5} & 0 & \frac{3}{5} & 0 & \dots & \dots & 0 \\ 0 & 0 & \frac{3}{7} & 0 & \frac{4}{7} & \dots & \dots & 0 \\ \vdots & & & & \ddots & \ddots & \vdots & \\ 0 & 0 & 0 & 0 & \dots & \frac{n-1}{2n-1} & 0 & \frac{n}{2n-1} \\ 0 & 0 & 0 & 0 & \dots & 0 & \frac{n}{2n+1} & 0 \end{pmatrix}, \tag{3.14}$$

$$\mathscr{C} = \tau^{-1} \begin{pmatrix} F_0 \\ -F_1 - 2f_1 \\ -5F_2 - 6f_2 \\ \vdots \\ -(n^2+n-1)F_n - n(n+1)f_n \end{pmatrix}.$$

With the exception of the source term $\mathscr{C}$, (3.13) is identical to the large angle scattering model of Paper 1.

The characteristic equation $|\mathscr{A} - \lambda \mathbf{I}| = 0$ yields the $(n+1)$ characteristics of (3.13), all of which are distinct. The characteristic speeds of the nth order truncation correspond to the 'speeds' into which the particles are scattered. In particular, for isotropic scattering models, we showed in Paper 1 that even-order truncations were inherently more accurate than odd-order truncations of the polynomial expanded Boltzmann equation. This is a consequence of the even-order truncations admitting $n/2$ forward and $n/2$ backward propagating characteristics and a single stationary characteristic. For the odd-order truncations, the stationary characteristic is always absent and, as a result, the odd-order truncations can never accurately capture particle propagation for particles with pitch-angles close to zero, i.e. nearly stationary scattered particles, no matter how refined. Since increasing the truncation order increases the number of characteristic speeds into which the particle distribution can be scattered, a higher-order truncation increases the accuracy of the solution. However, we found that, provided we used an even-order truncation, low-order polynomial expansions proved remarkably accurate with, for example, an f_2 approximation giving results almost identical to a higher-order f_4 approximation. This only is true, however, if the propagating source method is utilized.

Since the truncated Boltzmann equation reduced to a system of linear hyperbolic equations, the very powerful and accurate numerical method of characteristics is ideally suited to solve the equations. This has proved relatively straightforward to implement and yields accurate results.

3.2. Case $q = 2$

This case is particularly pertinent to cometary (Galeev and Sagdeev 1988; Glassmeier et al. 1989) and interstellar (Lee and Ip 1987; Williams and Zank 1994)

https://doi.org/10.1017/S0022377803002745 Published online by Cambridge University Press

pickup ions since quasi-linear theory predicts that the excited turbulence forms a k^{-2} spectrum. The pitch-angle diffusion coefficient (2.2) becomes

$$D_{\mu\mu}(\mu,\tau)=\frac{|\mu|(1-\mu^2)}{\tau}. \tag{3.15}$$

Observations of pickup ions (Fisk et al. 1997; Gloeckler and Geiss 1998) show anisotropic velocity distributions, which have been modeled (Isenberg 1997; Schwadron 1998; Lu and Zank 2001) by assuming that scattering from one hemisphere to the other proceeds much more slowly than scattering within each hemisphere. Clearly, from the non-isotropic diffusion coefficient $D_{\mu\mu}$ above, $D_{\mu\mu}=0$ at $\mu=0$ and scattering through 90° is therefore singular. As discussed above, the resonance gap at 90° is large when $q=2$, and other physics are needed to scatter particles from one hemisphere to the other. Accordingly, we consider the four models listed in Table 1.

*Model 1.*Mirroring and large-angle scattering can be included by introducing anisotropic relaxation time scattering operators, as considered in Paper 1, Lu and Zank (2001) and Lu et al. (2001). We therefore introduce distributions $f^{\pm}$ that correspond to the $\mu>0$ and $\mu<0$ hemispheres, respectively, and solve the generalization of (1.2):

$$\frac{\partial f^{\pm}}{\partial t}+\mu v\frac{\partial f^{\pm}}{\partial r}=\pm\frac{\partial}{\partial\mu}\left[\frac{\mu(1-\mu^2)}{\tau_1}\frac{\partial f^{\pm}}{\partial\mu}\right]+\frac{\langle f^{\mp}\rangle-f^{\pm}}{\tau_2}. \tag{3.16}$$

The mirroring/large-angle scattering rate τ_2^{-1} is much slower than the QLT scattering time τ_1^{-1}. Thus, pitch-angle scattering occurs in each hemisphere, independently of the other, and a slower scattering from one hemisphere to the other is controlled by the relaxation time operator.

As discussed above, we again split f into scattered and unscattered particles $f^{\pm}=F^{\pm}+f^{s\pm}$ to obtain

$$\frac{\partial F^{\pm}}{\partial t}+\mu v\frac{\partial F^{\pm}}{\partial r}=-\frac{F^{\pm}}{\bar\tau} \tag{3.17}$$

$$\frac{\partial f^{s\pm}}{\partial t}+\mu v\frac{\partial f^{s\pm}}{\partial r}=\pm\frac{\partial}{\partial\mu}\left[\frac{\mu(1-\mu^2)}{\tau_1}\frac{\partial f^{s\pm}}{\partial\mu}\right]\pm\frac{\partial}{\partial\mu}\left[\frac{\mu(1-\mu^2)}{\tau_1}\frac{\partial F^{\pm}}{\partial\mu}\right]+\frac{\langle f^{S\mp}\rangle-f^{s\pm}}{\tau_2}+\frac{\langle F^{\mp}\rangle}{\tau_2}+\frac{F^{\pm}}{\tau_1}, \tag{3.18}$$

where the averaged scattering time $\bar\tau^{-1}\equiv\tau_1^{-1}+\tau_2^{-1}$ has been introduced. Evidently,

$$F^{\pm}(r,t,\mu,v)=F^{\pm}(r-\mu vt,0,\mu,v)e^{-t/\bar\tau}. \tag{3.19}$$

We solve (3.18) using a half-range Legendre polynomial expansion

$$f^{s\pm}(r,t,\mu,v)=\sum_{n=0}^{\infty}(2n+1)P_n(2\mu\mp1)f_n^{\pm}(r,t,v),$$

$$f_n^{+}(r,t,v)=\frac{1}{2}\int_0^1 P(2\mu-1)f^{s+}(r,t,\mu,v)\,d\mu,$$

$$f_n^{-}(r,t,v)=\frac{1}{2}\int_{-1}^0 P(2\mu+1)f^{s-}(r,t,\mu,v)\,d\mu.$$

https://doi.org/10.1017/S0022377803002745 Published online by Cambridge University Press

The combined pitch-angle diffusion and large-angle scattering model then yields the infinite set of linear hyperbolic partial differential equations for the forward and backward harmonics $f_n^{\pm}$:

$$\begin{aligned}\frac{\partial f_n^{\pm}}{\partial t} + \frac{(n+1)v}{2(2n+1)}\frac{\partial f_{n+1}^{\pm}}{\partial r} \pm \frac{v}{2}\frac{\partial f_n^{\pm}}{\partial r} + \frac{nv}{2(2n+1)}\frac{\partial f_{n-1}^{\pm}}{\partial r}\\ = \mp\frac{n(n^2-1)}{2(2n+1)}\frac{f_{n-1}^{\pm}+F_{n-1}^{\pm}}{\tau_1} - \frac{3n(n+1)}{2}\frac{f_n^{\pm}+F_n^{\pm}}{\tau_1}\\ \mp\frac{n(n+1)(n+2)}{2(2n+1)}\frac{f_{n+1}^{\pm}+F_{n+1}^{\pm}}{\tau_1} + \frac{F_n^{\pm}}{\tau_1} - \frac{f_n^{\pm}}{\tau_2} + \delta_{n0}\frac{F_0^{\mp}+f_0^{\mp}}{\tau_2}\end{aligned} \tag{3.20}$$

where $\delta_{ij} = 0$ $(i \neq j)$ or 1 $(i = j)$.

The f_2 truncation of (3.20) can again be expressed as

$$\Psi_t + v\mathscr{A}\Psi_r = \mathscr{C} \tag{3.21}$$

with $\Psi = (f_0^-, f_0^+, f_1^-, f_1^+, f_2^-, f_2^+)^{\mathrm{T}}$ and the tridiagonal matrix

$$\mathscr{A} = \begin{pmatrix} -\frac{1}{2} & 0 & \frac{1}{2} & 0 & 0 & 0 \\ 0 & \frac{1}{2} & 0 & \frac{1}{2} & 0 & 0 \\ \frac{1}{6} & 0 & -\frac{1}{2} & 0 & \frac{1}{3} & 0 \\ 0 & \frac{1}{6} & 0 & \frac{1}{2} & 0 & \frac{1}{3} \\ 0 & 0 & \frac{1}{5} & 0 & -\frac{1}{2} & 0 \\ 0 & 0 & 0 & \frac{1}{5} & 0 & \frac{1}{2} \end{pmatrix},$$

$$\mathscr{C} = \begin{pmatrix} \frac{F_0^-}{\tau_1} - \frac{f_0^-}{\tau_2} + \frac{F_0^+ + f_0^+}{\tau_2} \\ \frac{F_0^+}{\tau_1} - \frac{f_0^+}{\tau_2} + \frac{F_0^- + f_0^-}{\tau_2} \\ -2\frac{F_1^-}{\tau_1} - 3\frac{f_1^-}{\tau_1} - \frac{f_1^-}{\tau_2} + \frac{F_2^- + f_2^-}{\tau_1} \\ -2\frac{F_1^+}{\tau_1} - 3\frac{f_1^+}{\tau_1} - \frac{f_1^+}{\tau_2} - \frac{F_2^+ + f_2^+}{\tau_1} \\ -8\frac{F_2^-}{\tau_1} - 9\frac{f_2^-}{\tau_1} - \frac{f_2^-}{\tau_2} + \frac{3}{5}\frac{F_1^- + f_1^-}{\tau_1} \\ -8\frac{F_2^+}{\tau_1} - 9\frac{f_2^+}{\tau_1} - \frac{f_2^+}{\tau_2} - \frac{3}{5}\frac{F_1^+ + f_1^+}{\tau_1} \end{pmatrix}. \tag{3.22}$$

The f_1 truncation (i.e. setting $f_2^{\pm} = 0$ above) admits the four characteristic speeds $\lambda_{\pm}^{\pm} = \pm\frac{1}{2}v(1 \pm \sqrt{\frac{1}{3}})$ and the f_2 truncation admits the six characteristics $\lambda_{\pm}^{0} = \pm\frac{1}{2}v$ and $\lambda_{\pm}^{\pm} = \pm\frac{1}{2}v(1 \pm \sqrt{\frac{3}{5}})$.No fundamentally different characteristic speeds are

https://doi.org/10.1017/S0022377803002745 Published online by Cambridge University Press

introduced in going from an odd to an even truncation for the half-range expansion and the decomposition simply becomes increasingly refined with increasing truncation order.

Before considering Models 2, 3 and 4, and our final example, $q=\frac{5}{3}$, we derive the 'diffusive' reduction of (3.21) at the f_1 truncation level. If gradients in $f_1^{\pm}$ are small, then

$$f_1^{\pm} \approx -\frac{v}{6}\frac{\tau_1\tau_2}{\tau_1+3\tau_2}\frac{\partial f_0^{\pm}}{\partial r} - 2\frac{\tau_2}{\tau_1+3\tau_2}F_1^{\pm}$$

which yields the coupled diffusion transport equations

$$\frac{\partial f_0^{\pm}}{\partial t} \pm \frac{v}{2}\frac{\partial f_0^{\pm}}{\partial r} + \frac{f_0^{\pm}+f_0^{\mp}}{\tau_2} = \frac{v^2}{12}\frac{\tau_1\tau_2}{\tau_1+3\tau_2}\frac{\partial^2 f_0^{\pm}}{\partial r^2} + \frac{F_0^{\pm}}{\tau_1} + \frac{F_0^{\mp}}{\tau_2} + \frac{\tau_2 v}{\tau_1+3\tau_2}\frac{\partial F_1^{\pm}}{\partial r}. \quad (3.23)$$

The slow large-angle scattering time τ_2 acts as a coupling coefficient between the forward and backward hemispheres. The coupling term in (3.23) is formally identical (when $\tau_2 \to \tau_1\tau_*/(\tau_1-2\tau_*)$) to the coupled term in diffusion transport equations (3.14) and (3.15) derived in Paper 1 on the basis of an anisotropic relaxation time scattering operator instead of $D_{\mu\mu}$.

3.3. *Case* $q=\frac{5}{3}$

The power spectrum of magnetic fluctuations in the interplanetary medium is frequently a broken power law with an inertial range exponent of $-\frac{5}{3}$; the Kolmogorov exponent for fully developed turbulence. If we assume that the particles scatter only with fluctuations in the inertial range of the magnetic fluctuation spectrum (see Bieber et al. (1994), Zank et al. (1998) and le Roux et al. (1999) for some discussion about particle scattering in the energy containing range), we can extend the approach above to investigate particle transport using the pitch-angle diffusion coefficient (2.2). Recall that for $q=\frac{5}{3}$, scattering through 90° is possible but slow. We either assume that some other physics control scattering through 90° or that we can approximate

$$\frac{f(0\pm)-f(0\mp)}{\tau} \approx \frac{\langle f^{\pm}\rangle - f^{\mp}}{\tau}$$

for some long scattering time parameter τ and $f(0\pm)$ denotes the particle distribution function immediately on either side of $\mu=0$.

We again use a half-range expansion and separate the distribution into scattered and unscattered particles. Although we omit the details, we note that the half-range expansion is particularly well suited to dealing with fractional powers $q-1$. Since the half-range expansion is in terms of Legendre polynomials with argument $2\mu\pm1$, the variable $\xi=2\mu\pm1$ allows us to replace $|\mu|^{q-1}$ by a term proportional to $|\xi\mp1|^{q-1}$. A binomial expansion of the fractional term to the desired order (chosen to be consistent with the level of truncation for the resulting infinite set of partial differential equations (PDEs)) and repeated use of the various Legendre polynomial recursion relations allows us to follow a procedure similar to that of Sec. 3.2. In doing so, we obtain the infinite set of equations in the harmonics $f_n^{\pm}$, where for the present we have assumed Model 1 of Table 1,

$$\frac{\partial f_n^{\pm}}{\partial t} + \frac{(n+1)v}{2(2n+1)}\frac{\partial f_{n+1}^{\pm}}{\partial r} \pm \frac{v}{2}\frac{\partial f_n^{\pm}}{\partial r} + \frac{nv}{2(2n+1)}\frac{\partial f_{n-1}^{\pm}}{\partial r} = \frac{F_n^{\pm}}{\tau_1} - \frac{f_n^{\pm}}{\tau_2} + \delta_{n0}\frac{F_0^{\mp}+f_0^{\mp}}{\tau_2} + Q_n^{\pm} \quad (3.24)$$

https://doi.org/10.1017/S0022377803002745 Published online by Cambridge University Press

where

$$
\begin{aligned}
Q_n^{\pm} = \frac{n(n+1)}{\sqrt[3]{4}}\Bigg\{ & -3\frac{f_n^{\pm}+F_n^{\pm}}{\tau_1} + \frac{2n^2+2n-3}{3(2n-1)(2n+3)}\frac{f_n^{\pm}+F_n^{\pm}}{\tau_1} \\
& - \frac{(n+2)(n+3)}{3(2n+1)(2n+3)}\frac{f_{n+2}^{\pm}+F_{n+2}^{\pm}}{\tau_1} - \frac{(n-2)(n-1)}{3(2n-1)(2n+1)}\frac{f_{n-2}^{\pm}+F_{n-2}^{\pm}}{\tau_1} \\
& \pm \frac{8}{9}\frac{(n-1)(n^2-3)}{(2n-3)(2n+1)(2n+3)}\frac{f_{n-1}^{\pm}+F_{n-1}^{\pm}}{\tau_1} \\
& \pm \frac{8}{9}\frac{(n+2)(n^2+2n-2)}{(2n-1)(2n+1)(2n+5)}\frac{f_{n+1}^{\pm}+F_{n+1}^{\pm}}{\tau_1} \\
& \pm \frac{8}{27}\frac{(n+2)(n+3)(n+4)}{(2n+1)(2n+3)(2n+5)}\frac{f_{n+3}^{\pm}+F_{n+3}^{\pm}}{\tau_1} \\
& \pm \frac{8}{27}\frac{(n-1)(n-2)(n-3)}{(2n-3)(2n-1)(2n+1)}\frac{f_{n-3}^{\pm}+F_{n-3}^{\pm}}{\tau_1}\Bigg\}. \qquad (3.25)
\end{aligned}
$$

Since the f_2 truncation is used in the results below, the reduction of (3.24) and (3.25) in the small-angle scattering case is given by

$$
\begin{aligned}
\frac{\partial f_0^{\pm}}{\partial t} + v\frac{\partial f_1^{\pm}}{\partial r} \pm \frac{v}{2}\frac{\partial f_0^{\pm}}{\partial r} &= \frac{F_0^{\pm}}{\tau} \\
\frac{\partial f_1^{\pm}}{\partial t} + \frac{v}{3}\frac{\partial f_2^{\pm}}{\partial r} \pm \frac{v}{2}\frac{\partial f_1^{\pm}}{\partial r} + \frac{v}{6}\frac{\partial f_0^{\pm}}{\partial r} &= \frac{F_1^{\pm}}{\tau} - \frac{46\sqrt[3]{2}}{15}\frac{F_1^{\pm}+f_1^{\pm}}{\tau} \pm \frac{8\sqrt[3]{2}}{63}\frac{F_2^{\pm}+f_2^{\pm}}{\tau} \\
\frac{\partial f_2^{\pm}}{\partial t} \pm \frac{v}{2}\frac{\partial f_2^{\pm}}{\partial r} + \frac{v}{5}\frac{\partial f_1^{\pm}}{\partial r} &= \frac{F_2^{\pm}}{\tau} - \frac{66\sqrt[3]{2}}{7}\frac{F_2^{\pm}+f_2^{\pm}}{\tau} \pm \frac{8\sqrt[3]{2}}{105}\frac{F_1^{\pm}+f_1^{\pm}}{\tau}. \qquad (3.26)
\end{aligned}
$$

Consider now the remaining models listed in Table 1. For Models 2, 3 and 4, the transport equation that we need to solve may be expressed as

$$
\frac{\partial f}{\partial t} + \mu v\frac{\partial f}{\partial r} = \frac{\partial}{\partial \mu}\left[\frac{(|\mu|^{q-1}+\epsilon)(1-\mu^2)}{\tau}\frac{\partial f}{\partial \mu}\right], \qquad (3.27)
$$

where ϵ denotes the parameter for particle scattering through 90°. Equation (3.27) is a little more difficult to solve than the relaxation time models and we are obliged to introduce an operator splitting method. To this end, we first solve

$$
\frac{\partial f^{\pm}}{\partial t} + \mu v\frac{\partial f^{\pm}}{\partial r} = \frac{\partial}{\partial \mu}\left[\frac{|\mu|^{3/2}(1-\mu^2)}{\tau}\frac{\partial f^{\pm}}{\partial \mu}\right], \qquad (3.28)
$$

where, as before, we separate the distribution into forward and backward moving particles and $q = \frac{5}{3}$. Again, we introduce a scattered and unscattered particle decomposition, use a half-range Legendre polynomial expansion and derive an infinite set of linear hyperbolic PDEs

$$
\frac{\partial f_n^{\pm}}{\partial t} + \frac{(n+1)v}{2(2n+1)}\frac{\partial f_{n+1}^{\pm}}{\partial r} \pm \frac{v}{2}\frac{\partial f_n^{\pm}}{\partial r} + \frac{nv}{2(2n+1)}\frac{\partial f_{n-1}^{\pm}}{\partial r} = \frac{F_n^{\pm}}{\tau} + Q_n^{\pm}. \qquad (3.29)
$$

https://doi.org/10.1017/S0022377803002745 Published online by Cambridge University Press

The f_2 approximation is given by

$$\frac{\partial f_0^{\pm}}{\partial t} + v\frac{\partial f_1^{\pm}}{\partial r} \pm \frac{v}{2}\frac{\partial f_0^{\pm}}{\partial r} = \frac{F_0^{\pm}}{\tau}$$

$$\frac{\partial f_1^{\pm}}{\partial t} + \frac{v}{3}\frac{\partial f_2^{\pm}}{\partial r} \pm \frac{v}{2}\frac{\partial f_1^{\pm}}{\partial r} + \frac{v}{6}\frac{\partial f_0^{\pm}}{\partial r} = \frac{F_1^{\pm}}{\tau} - \frac{46\sqrt[3]{2}}{15}\frac{F_1^{\pm} + f_1^{\pm}}{\tau} \pm \frac{8\sqrt[3]{2}}{63}\frac{F_2^{\pm} + f_2^{\pm}}{\tau}$$

$$\frac{\partial f_2^{\pm}}{\partial t} \pm \frac{v}{2}\frac{\partial f_2^{\pm}}{\partial r} + \frac{v}{5}\frac{\partial f_1^{\pm}}{\partial r} = \frac{F_2^{\pm}}{\tau} - \frac{66\sqrt[3]{2}}{7}\frac{F_2^{\pm} + f_2^{\pm}}{\tau} \pm \frac{8\sqrt[3]{2}}{105}\frac{F_1^{\pm} + f_1^{\pm}}{\tau}. \quad (3.30)$$

Having solved the first part of the operator split (3.33), we then solve

$$\frac{\partial f}{\partial t} + \mu v\frac{\partial f^{\pm}}{\partial r} = \frac{\partial}{\partial \mu}\left[\frac{\epsilon(1-\mu^2)}{\tau}\frac{\partial f^{\pm}}{\partial \mu}\right] \quad (3.31)$$

and this equation applies only to the scattered particles. Equation (3.31) is solved straightforwardly using a regular Legendre polynomial expansion, yielding

$$f_n' = f_n \exp\left[-n(n+1)\frac{\epsilon \Delta t}{\tau}\right] \quad (3.32)$$

where f_n' denotes the updated value and f_n is the value contributed by solving (3.30) (but expressed in terms of the expansion used to solve (3.31) and not the half-range expansion used in the previous split). The updated value f_n' must then be re-expressed in terms of the half-range expansion used to solve (3.28), which leads to an attractive set of relations between the operator split relations (not reproduced here).

4. Relaxation time versus pitch-angle diffusion scattering operators

Our purpose in this section is to compare the large-angle relaxation time scattering operator with the pitch-angle diffusion form of the scattering operator. We consider both isotropic (i.e. a single-time relaxation operator and the diffusion operator with $q = 1$) and anisotropic scattering models (i.e. a two-time relaxation operator and the diffusion operator with $q \neq 1$).

To solve the various sets of truncated equations, we implement the method of characteristics numerically. As an initial condition, we assume a ring beam distribution (3.3) which is spatially localized between $r = 0$ and $r = r_0$ such that

$$N(r) = H(r) - H(r - r_0),$$

where $H(r)$ denotes the Heaviside step function. In the calculations, we always use normalized values always, so that $r_0 = 1$, $v = v_0 = 1$ and $\mu_0 = 0.6$. Unless we are using an anisotropic scattering model for the relaxation time operator, we use $\tau = 1$.

4.1. Isotropic scattering

Equation (1.2) is solved with either the relaxation time scattering operator (2.3) or the quasi-linear operator with $q = 1$. The explicit form of the truncated equations for the single time relaxation model can be found in (2.16) of Paper 1, and the truncated system (3.13) is used for the quasi-linear solutions. Figure 1 shows the scattered component f_s of the distribution function corresponding to f_1 and f_2 truncations of both scattering models. Figure 1 directly compares the evolution of an identical initial ring beam using (a) a single time relaxation scattering operator

https://doi.org/10.1017/S0022377803002745 Published online by Cambridge University Press

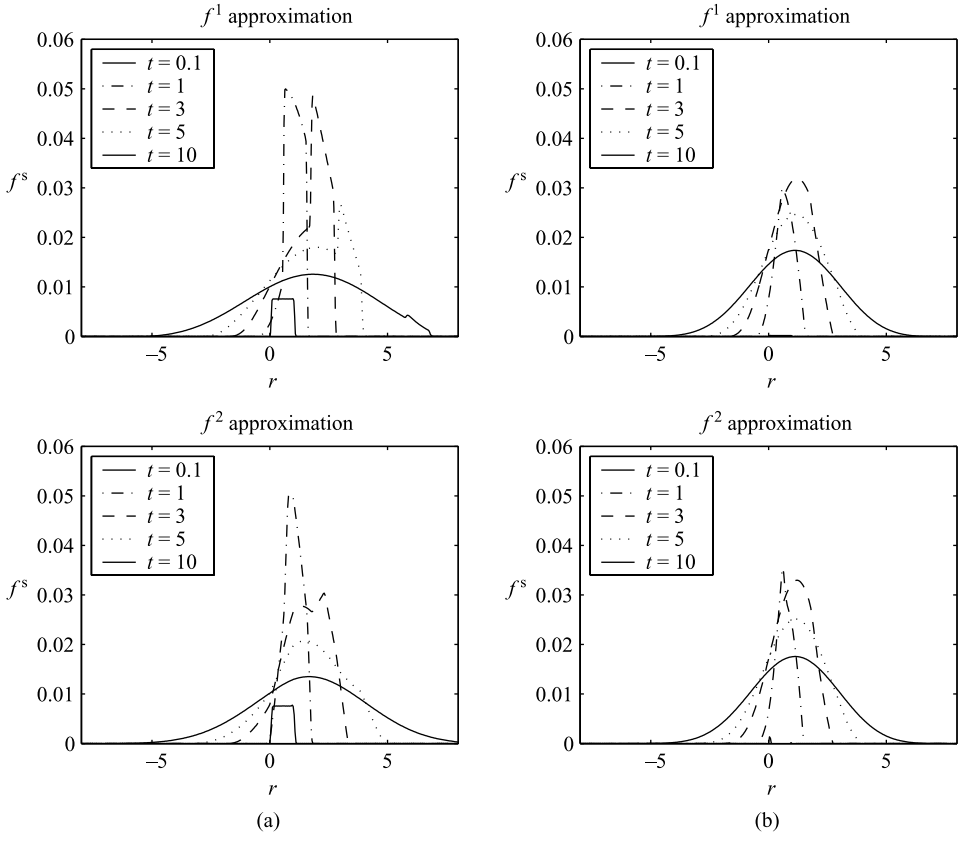

Figure 1. A comparison of solutions obtained using f_1 and f_2 truncations for (a) a single-time relaxation operator and (b) the $q = 1$ quasi-linear scattering operator. The scattered distribution f^s is plotted for normalized times $t = 0.1$ to 10. The plots are along $\mu = \mu_0 = 0.6$.

and (b) an isotropic $q = 1$ QLT scattering operator. Solutions are shown from an early time ($t/\tau = 0.1$) until a later time ($t/\tau = 10$). Noticeable in Fig. 1(b) is that the amplitude of the scattered particle distribution increases slowly despite the presence of higher-order source term harmonics F_n in the pitch-angle diffusion case. However, at later times (e.g. $t/\tau = 10$), the small-angle scattering model has diffused less than the large-angle scattering model and, consequently, the amplitude of the distribution function is high in the former. This, of course, is simply a consequence of large-angle scattering enabling greater access of all phase space than the small-angle scattering operator. Like the large-angle scattering case, no coherent pulses are present in both the f_1 or f_2 truncations.

Figure 2 illustrates the total distribution function $f = F + f^s$ as a function of position at times corresponding to those of Figure 1. As before, Fig. 2(a) corresponds to the relaxation time operator and Fig. 2(b) to the QLT operator. Evidently, at early times, the solution is dominated by the initial beam.

The contribution of the harmonics f_0, f_1 and f_2 to the total scattered distribution function f^s in the QLT model is illustrated in Fig. 3. The f_1 and f_2 truncations are shown for two times $t/\tau = 1$, 5 and $\mu = 0.6$. Like the large-angle scattering

https://doi.org/10.1017/S0022377803002745 Published online by Cambridge University Press

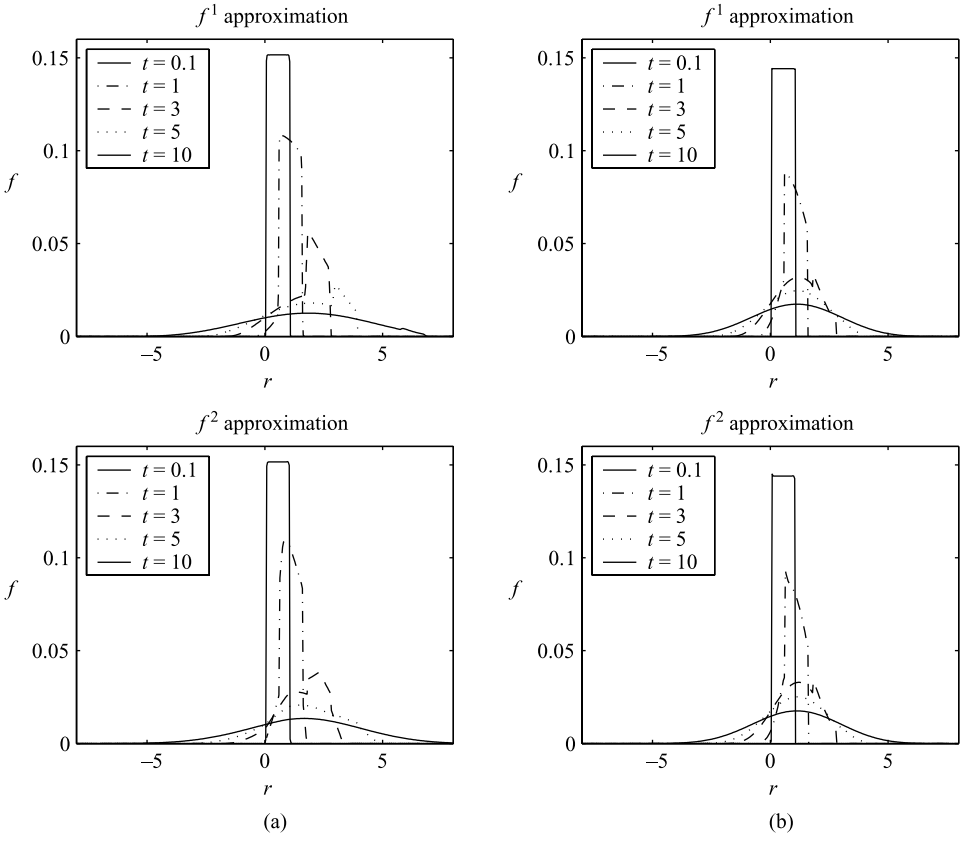

Figure 2. The total distribution $f = F + f^s$ as a function of position for times corresponding to those of Fig. 1 along $\mu = 0.6$. The f_1 and f_2 truncation of the single-time relaxation operator is shown in (a), while (b) represents the f_1 and f_2 truncations of $q = 1$ quasi-linear scattering operator.

case, the f_0 truncation dominates and the f_1 and f_2 harmonics are very similar in amplitude and spatial distribution to those of the large-angle model. Under these circumstances, expanding the distribution f_n about the isotropic distribution f_0 is valid, but this certainly need not be the case for anisotropic scattering model.

In Fig. 4, we plot the intensity profile for the total distribution function f for both the large-angle scattering and small-angle scattering operators. The values plotted are along $\mu = 0.6$. Two normalized spatial locations are chosen: $r = 1.3$ and 3.0. As is seen, the large-angle scattering exhibits a slightly higher amplitude. In this case, the peak of the amplitude is also reached earlier compared with the small-angle scattering. In the latter case, the decay in amplitude also occurs at a slower rate.

A comparison of the small-angle isotropic and large-angle isotropic scattering models presented here and in Paper 1 suggests that the two approaches do not yield qualitatively different results. The small-angle scattering operator leads to a slower spreading of the scattered particles and, consequently, intensity profiles can have slightly greater amplitudes at later times in this case. However, these differences are sufficiently slight so as to suggest that the simple relaxation time operator is a

https://doi.org/10.1017/S0022377803002745 Published online by Cambridge University Press

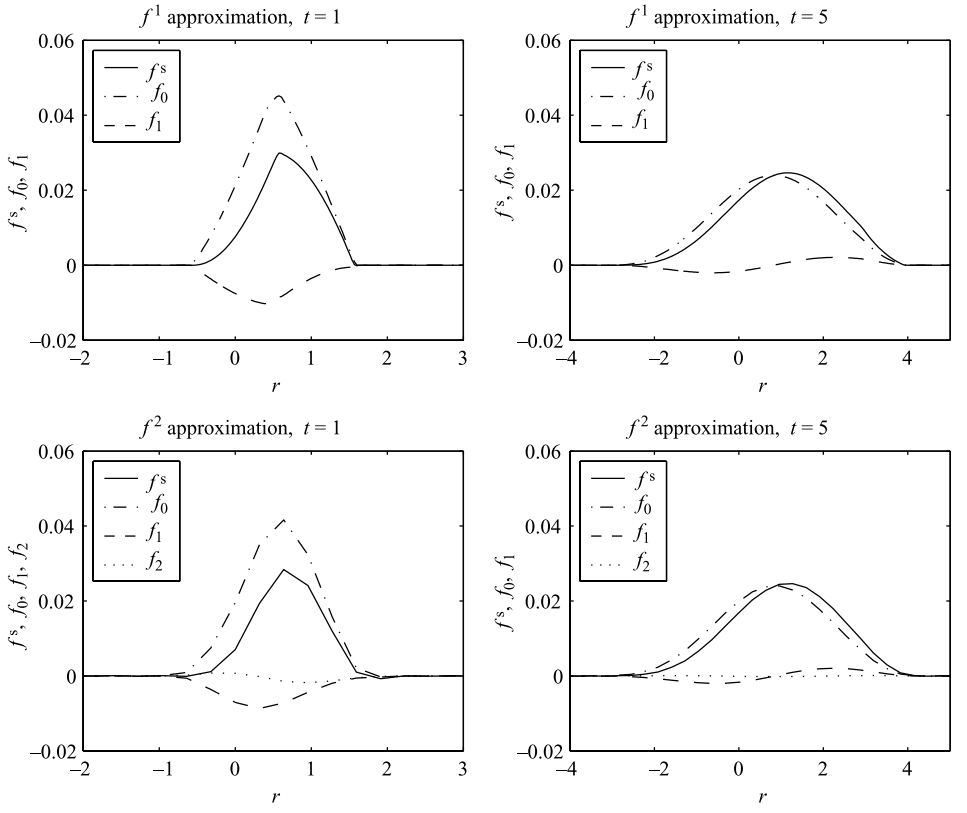

Figure 3. The contributions of the harmonics f_0 and f_1 to f^s in the f_1 approximation at normalized times $t/\tau = 1$ and 5 and the contribution of the harmonics f_0, f_1 and f_2 to f_s in the f_2 approximation at the same times. $\mu = 0.6$ for both cases. Only the $q = 1$ small angle scattering model is illustrated.

reasonable approximation to the simplest isotropic small-angle scattering operator (2.1) when $q = 1$.

4.2. Anisotropic scattering

As discussed above, one approach to incorporating the slow scattering of particles through 90° in the context of the relaxation time scattering operator is to introduce two scattering time scales τ_1 and τ_2. The first time scale describes the more rapid scattering within each hemisphere and the second describes the slower scattering of particles through 90°. In this section, we compare the two-time relaxation scattering model and the QLT pitch-angle diffusion model with $q = 2$. However, this immediately introduces the problem of scattering through 90° for the QLT model and so we use the mirroring model of Table 1. Two QLT cases are considered: the first corresponds to strong scattering of particles through 90°, for which $\tau_2 = 3\tau_1$; the second corresponds to weak scattering of particles through a zero pitch angle, with $\tau_2 = 10\tau_1$. In the strong-scattering model, scattering through 90° proceeds at almost the same rate as scattering within the hemispheres and the model is therefore very nearly isotropic in character. The second QLT model is evidently highly anisotropic.

https://doi.org/10.1017/S0022377803002745 Published online by Cambridge University Press

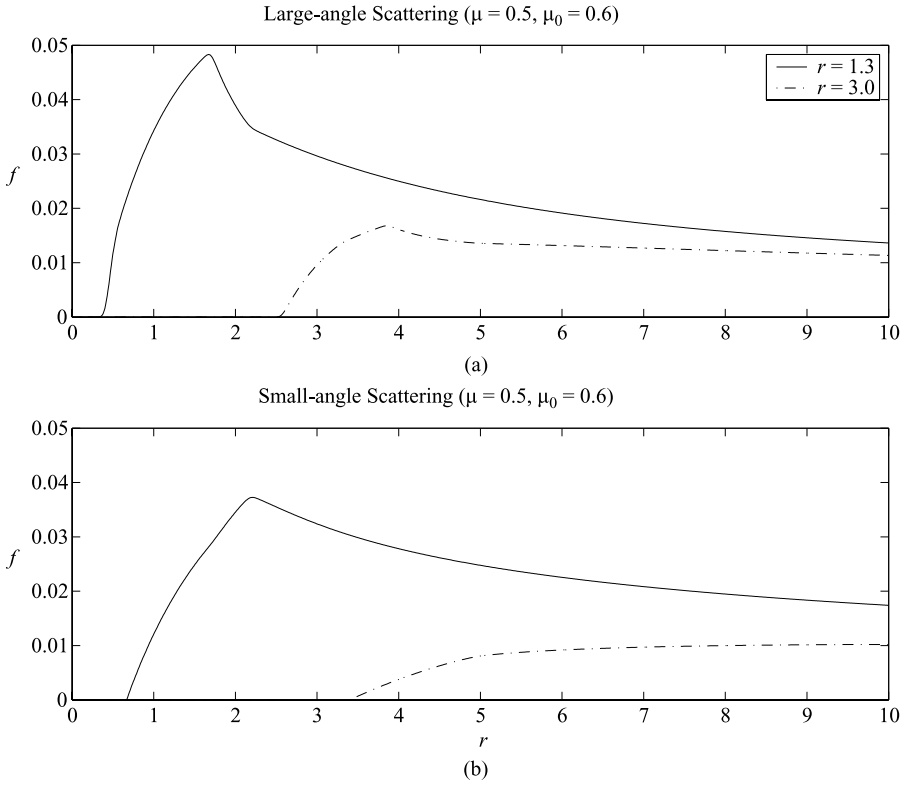

Figure 4. A plot of the distribution function f as a function of time for $\mu = 0.3$ at two (normalized) spatial locations $r = 1.3$ and 3.0 for (a) the large-angle scattering operator and (b) the QLT isotropic scattering operator.

Figures 5, 6 and 7 illustrate the temporal evolution of an initial ring beam distribution as a function of position subject to: (i) a weak scattering two-time relaxation operator with $\tau_2 = 10\tau_1$; (ii) a weak QLT scattering operator; and (iii) a strong QLT scattering model, respectively. All three cases use the f_2 truncation and measure the distribution evolution in terms of the normalized time $\bar{\tau}^{-1} = \tau_1^{-1} + \tau_2^{-1}$. The omnidirectional distribution is plotted, together with a decomposition into forward- and backward-hemisphere particles and scattered and unscattered particles.

The two weak scattering models illustrated in Figs 5 and 6 can be compared directly. At early times, both the relaxation time and QLT models are dominated by the propagating ring beam. A persistent pulse appears after about $t/\bar{\tau} \approx 1.5$ in both cases, but the pulse front of the QLT model lags behind that of the relaxation model from $t/\bar{\tau} = 1$. Apart from this, however, the character of the evolving distributions subject to two apparently quite different scattering models is surprisingly similar. At $t/\bar{\tau} = 10$, both scattering models exhibit a pronounced rightward moving pulse followed by a spatial tail, but the pulse front extends further out for the relaxation model. With some minor adjusting of the values of $\bar{\tau}$ in the relaxation models, we expect that the QLT and relaxation scattering models would be virtually indistinguishable.

https://doi.org/10.1017/S0022377803002745 Published online by Cambridge University Press

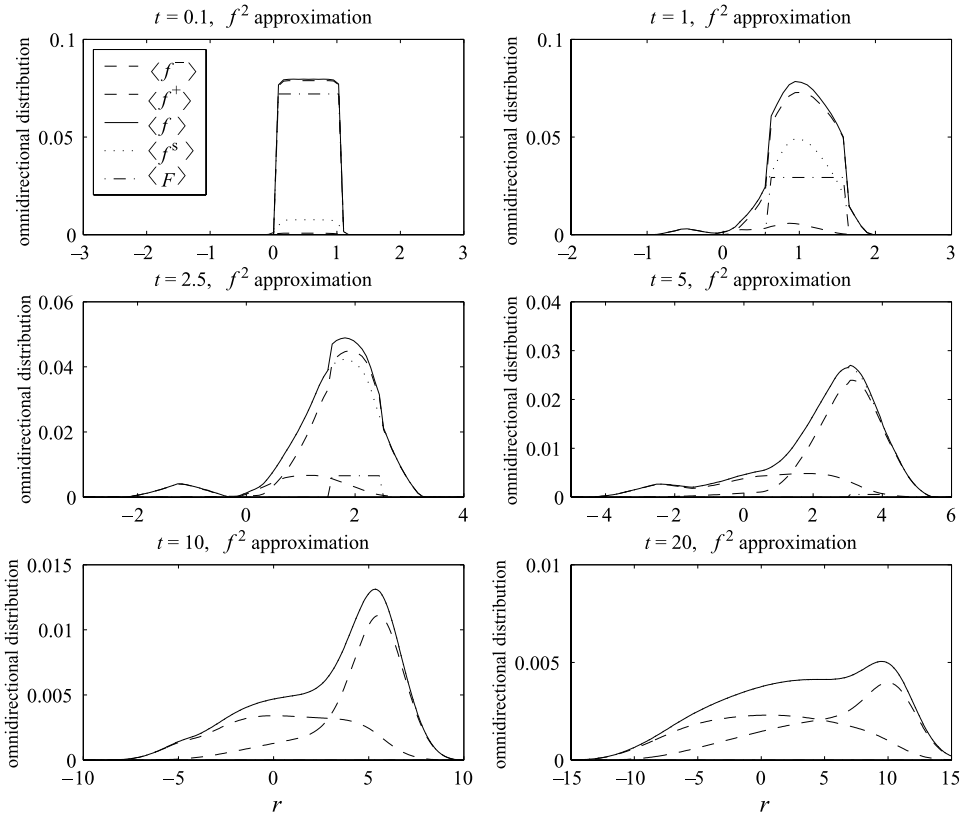

Figure 5. The temporal evolution of a single rightward-propagating ring beam for the normalized times $t/\tau = 0.1,\ 1,\ 2.5,\ 5,\ 10,\ 20$ in the weak scattering limit $\tau_2/\tau_1 = 10$ of the large-angle two-time relaxation model. The omnidirectional distribution function $\langle f \rangle$, the scattered distribution $\langle f^s \rangle$, the beam $\langle F \rangle$ and the forward- and backward-propagating distributions $\langle f^{\pm} \rangle$ are plotted. An f_2 truncation is used and all times are normalized to the scattering time $\bar{\tau}$.

The QLT strong scattering model illustrated in Fig. 7 evolves quite differently from the QLT weak scattering model. As before, the ring beam dominates at early times and a rightward-propagating pulse forms at the same normalized time. The leading pulse is, however, eroded much more rapidly in this case and a much more dominant leftward-propagating component is produced—this an obvious consequence of the particles ability to scatter rapidly from one hemisphere to the other. By $t/\bar{\tau} > 5$, the leading pulse has virtually disappeared and the spatial distribution soon acquires a normal character. The speed at which the distribution front propagates is, however, identical in both the weak and strong scattering models.

The major result to emerge from this section is that the single-time and two-time relaxation models do surprisingly well in describing the propagation and temporal evolution of beams, comparing very well to the QLT scattering models when mirroring is assumed to scatter particles through 90°. Some minor adjustment of relaxation scattering times would allow almost indistinguishable results to be achieved between the two approaches.

https://doi.org/10.1017/S0022377803002745 Published online by Cambridge University Press

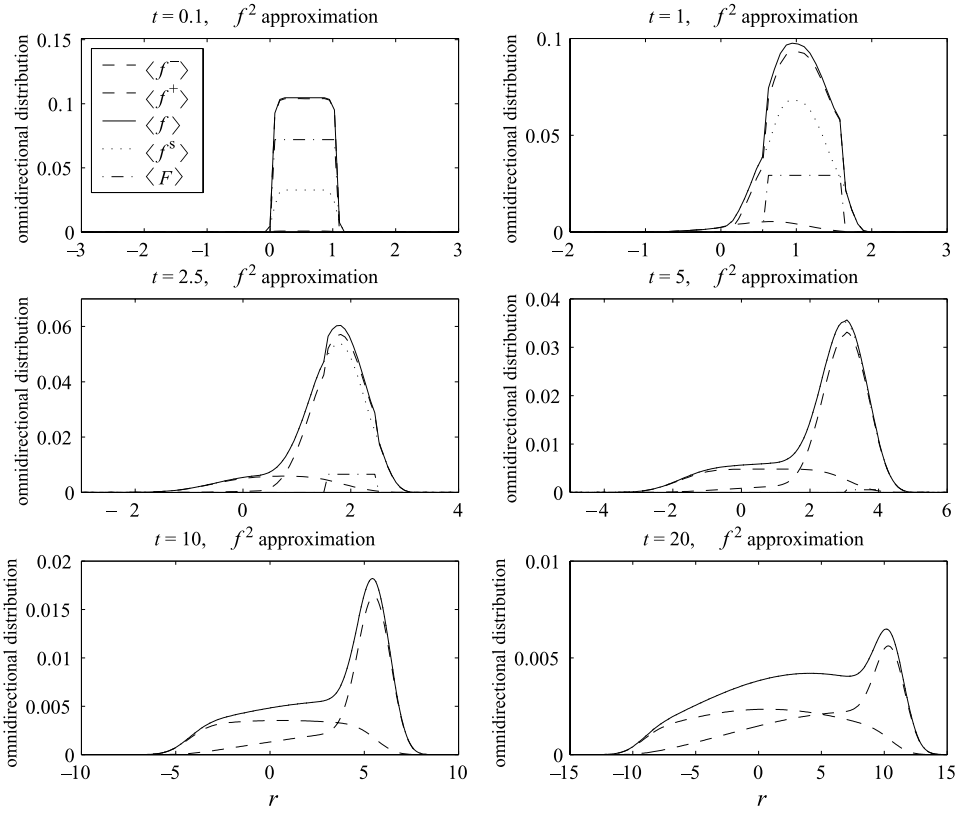

Figure 6. The temporal evolution of a right-propagating ring beam for the normalized times $t/\tau = 0.1$, 1, 2.5, 5, 10, 20 in the weak scattering limit $\tau_2/\tau_1 = 10$ of the small-angle anisotropic QLT $q = 2$ model in the presence of large angle mirroring (Model 1 in Table 1). The omnidirectional distribution function $\langle f \rangle$, the scattered distribution $\langle f^s \rangle$, the beam $\langle F \rangle$ and the forward- and backward-propagating distributions $\langle f^{\pm} \rangle$ are plotted. An f_2 truncation is used and all times are normalized to the scattering time $\bar{\tau}$.

In concluding this section, we present in Fig. 8 a comparison of intensity profiles for three QLT models with weak mirroring, using values of $q = 1$, $\frac{5}{3}$ and 2. The plots are for a pitch angle of $\mu = 0.5$ and a position of $r = 2$. Although the arrival times are almost identical for all three scattering models, the arrival time of the total distribution function f peak for the $q = 1$ case is as much as a diffusion time later than the arrival time for the other two cases (which are virtually coincident). Since the initial pitch angle $\mu_0 = 0.6$ and the scattering from one hemisphere is weak, the more anisotropic distributions associated with the $q = \frac{5}{3}$ and 2 cases ensure that their peaks arrive sooner than the isotropic scattering model.

5. Quasi-linear models and scattering through 90°

In this section, we assume a Komlogorov turbulence model (i.e. $q = \frac{5}{3}$) exclusively and solve the Boltzmann equation (1.2) for Models 1–4 listed in Table 1. Thus, we assume the standard QLT expression (2.2) and augment it by a model that describes

https://doi.org/10.1017/S0022377803002745 Published online by Cambridge University Press

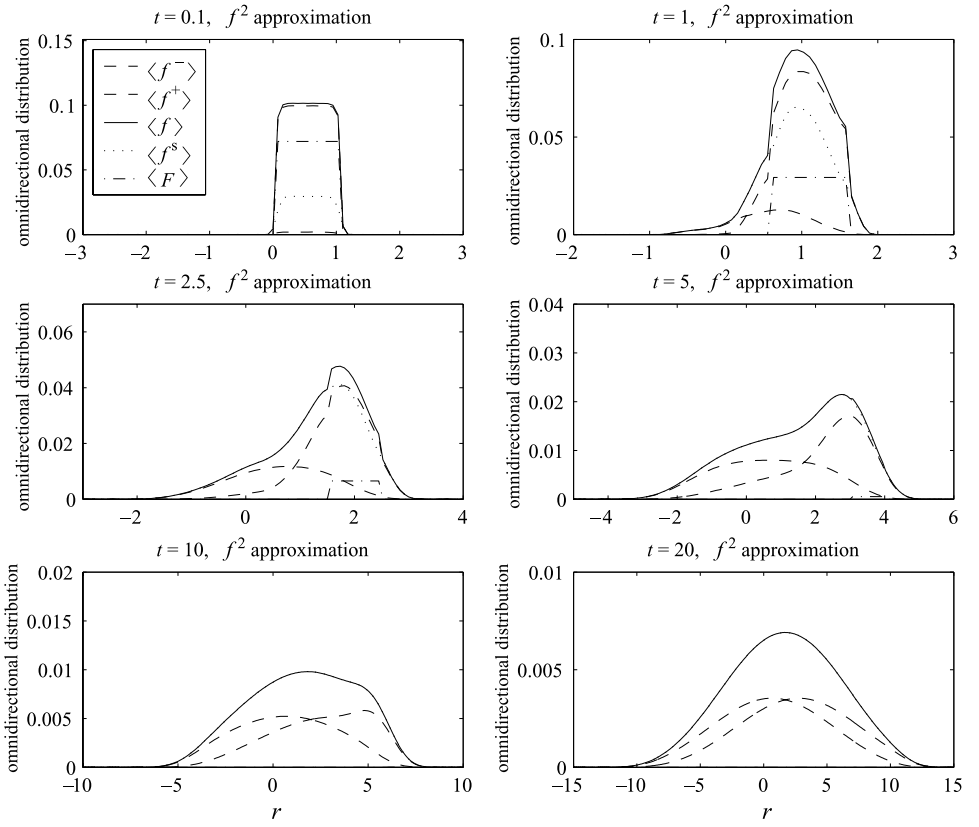

Figure 7. The temporal evolution of a right-propagating ring beam for the normalized times $t/\tau = 0.1$, 1, 2.5, 5, 10, 20 in the strong scattering limit $\tau_2/\tau_1 = 3$ of the small-angle anisotropic QLT $q = 2$ model in the presence of large angle mirroring (Model 1 in Table 1). The omnidirectional distribution function $\langle f \rangle$, the scattered distribution $\langle f^s \rangle$, the beam $\langle F \rangle$ and the forward- and backward-propagating distributions $\langle f^{\pm} \rangle$ are plotted. An f_2 truncation is used and all times are normalized to the scattering time $\bar{\tau}$.

scattering through 90°, such as large-angle mirroring, dynamical turbulence effects, or resonant and non-resonant scattering wave models.

Figures 9 and 10 compare two Model 1 examples (i.e. assuming that mirroring is responsible for scattering through 90°), one with a slow rate of scattering from one hemisphere to the other (ten times slower than the QLT scattering time or $\tau_2 = 10\tau_1$, Fig. 9) and the other with a fast rate (three times slower than the QLT scattering time or $\tau_2 = 3\tau_1$, Fig. 10).

The example illustrated in Fig. 9 is not significantly different from the $q = 2$ example of Fig. 7. Slight differences in detail are noticeable, but the minor modifications to (2.2) that result from using $q = \frac{5}{3}$ instead of $q = 2$ do not significantly affect the scattering rates. Similar comments hold for the differences between the strong scattering $q = \frac{5}{3}$ and 2 models. Clearly, however, large differences exist between models which admit strong and weak mirroring of particles through 90°. In the former case, a distinguishable rightward-propagating pulse is present until a little after $t/\tau = 5$ scattering times, but thereafter the distribution spreads out almost

https://doi.org/10.1017/S0022377803002745 Published online by Cambridge University Press

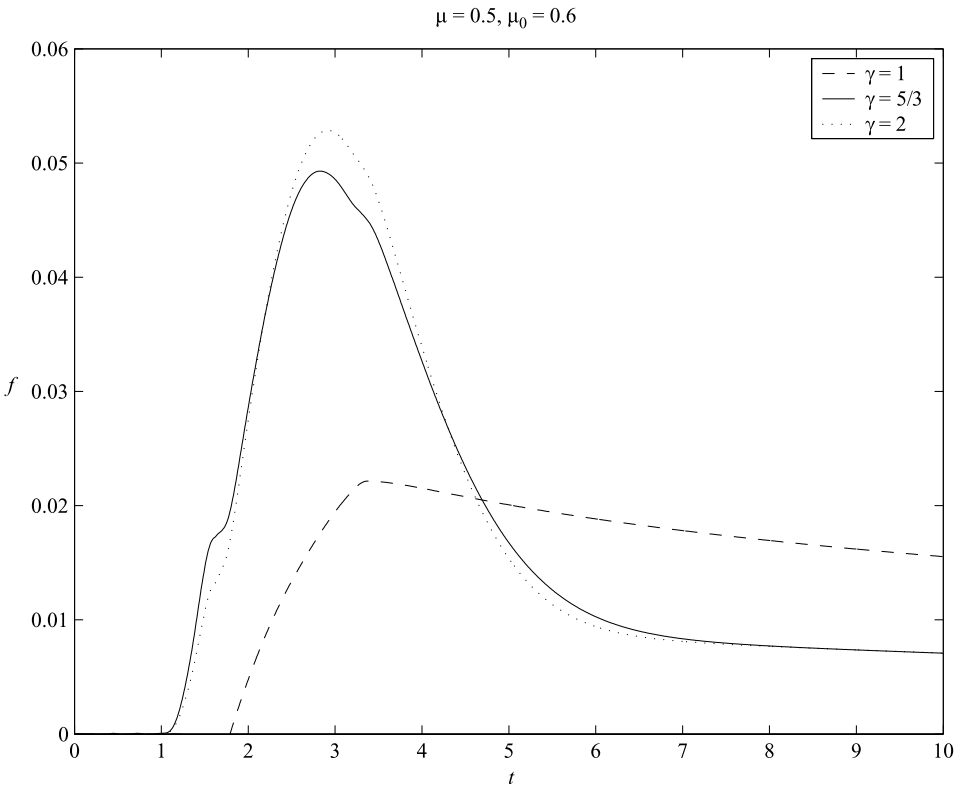

Figure 8. Intensity plots of the distribution function f observed at a given position $r = 2$ and pitch angle for three values of $q = 1$, $\frac{5}{3}$ and 2 for the QLT weak scattering model.

'diffusively' in both directions. The spatial distribution is approximately normally distributed in space after $t/\tau = 20$ scattering times, with a slow moving peak at $r = 1.5$. In contrast, the weak mirroring model admits a very pronounced rightward-propagating pulse, which, even after $t/\tau = 20$, is still present.

Although formally the same structurally, the dynamical turbulence and wave models, using either resonant or non-resonant scattering of particles through 90°, admit slightly different rates of scattering through $\mu = 0$. Accordingly, we have normalized the 90° resonant scattering time, the exit scattering time and the dynamical turbulence scattering time $\Phi(\mu = 0)$ to the QLT scattering time τ_1. Crudely, τ_1 will scale inversely with particle gyrofrequency and, as discussed by Ragot (1999), τ_{exit} also scales with or is less than the inverse particle gyrofrequency. Unlike the wave models, where the rate of scattering through 90° is determined primarily by the ratio of wave speed to particle speed, the dynamical turbulence model scattering rates are determined by the Eulerian frequency spectrum $G_{\text{E}}(\Omega)$ (Bieber et al. 1994). Bieber et al. (1994) compute, for the reduced perpendicular power spectrum of the slab model (their Fig. 5), an Eulerian frequency spectrum for both their damping and random sweeping models (their Fig. 6). Relativistic protons interact primarily with the inertial range of the turbulence spectrum, where $G_{\text{E}}(\Omega) \approx B\Omega^{-1.6}$. Thus, for relativistic protons (and highly relativistic electrons),

https://doi.org/10.1017/S0022377803002745 Published online by Cambridge University Press

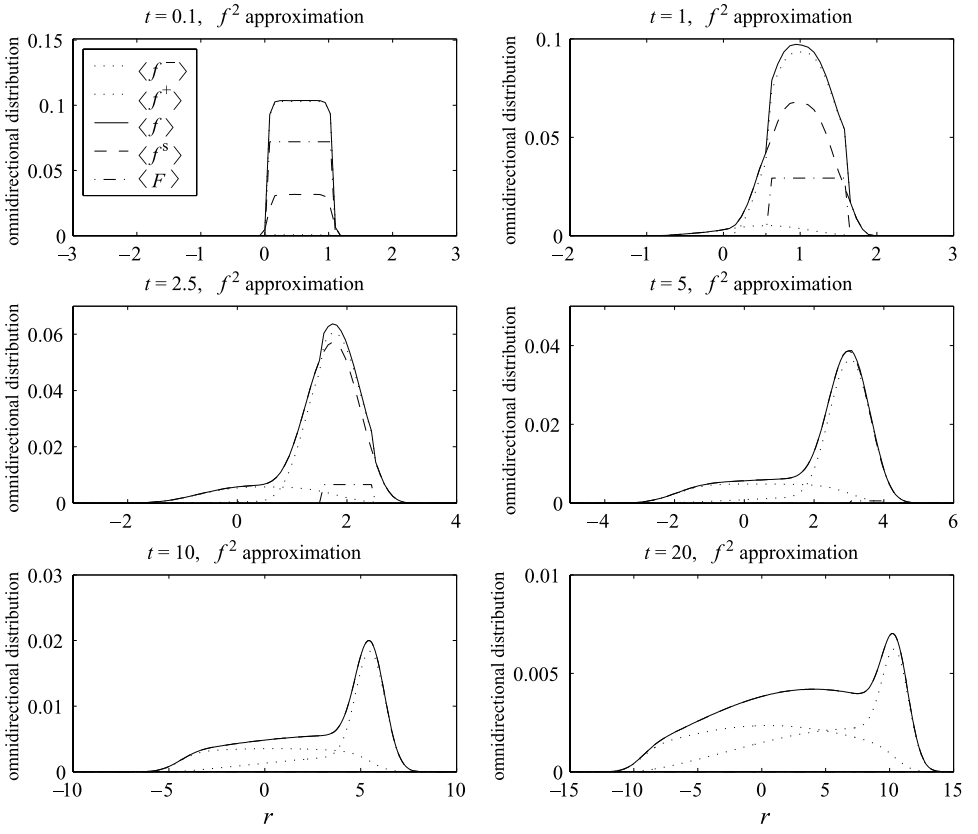

Figure 9. The temporal evolution of a right-propagating ring beam for the normalized times $t/\tau = 0.1,\ 1,\ 2.5,\ 5,\ 10,\ 20$ in the limit of weak mirroring ($\tau_2/\tau_1 = 10$) for the small-angle anisotropic QLT $q = \frac{5}{3}$ model (Model 1 in Table 1). The omnidirectional distribution function $\langle f \rangle$, the scattered distribution $\langle f^s \rangle$, the beam $\langle F \rangle$ and the forward- and backward-propagating distributions $\langle f^{\pm} \rangle$ are plotted. An f_2 truncation is used and all times are normalized to the scattering time $\bar{\tau}$.

the dynamical turbulence model implies that the normalized quantity

$$\tau_1 \Phi(\mu = 0) \approx \frac{8B}{Av^{0.06}} \Omega^{0.06} \tag{5.1}$$

is very weakly dependent on gyrofrequency. Extracting estimates for A and B from the graph of Bieber et al. (1994) yields values of the normalized scattering times for the perpendicular pitch-angle diffusion coefficient between about 0.1 and 0.01 for protons. For mildly relativistic electrons, still resonant with the dissipation range, the normalized quantity analogous to (5.1) can become much smaller than the corresponding proton value (of the order of $\sim 10^{-4}$ and less). For such electrons, the differences between the distribution functions obtained from the damping or random sweeping models do not appear to be large.

In view of the orderings discussed above and in Table 1, we considered three simulations. If we denote by ϵ the normalized parameter multiplying the $(1 - \mu^2)$

https://doi.org/10.1017/S0022377803002745 Published online by Cambridge University Press

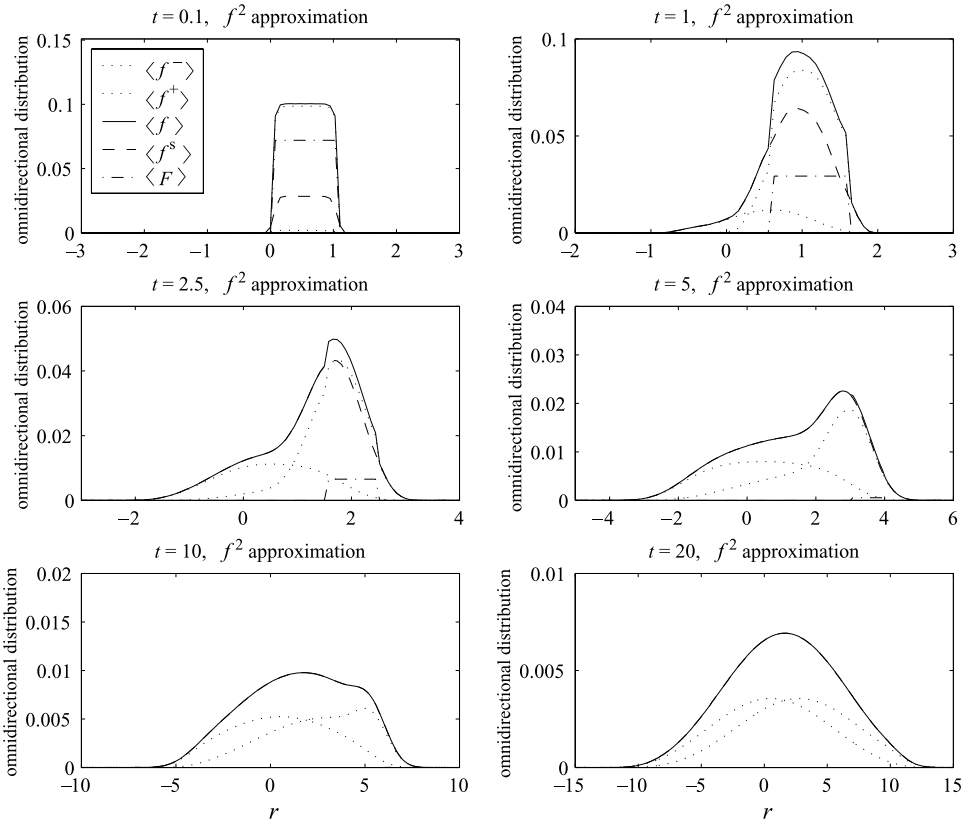

Figure 10. As Fig. 9, but now in the limit of strong mirroring ($\tau_2/\tau_1 = 3$) for the small-angle QLT $q = \frac{5}{3}$ model (Model 1 of Table 1). The omnidirectional distribution function $\langle f \rangle$, the scattered distribution $\langle f^s \rangle$, the beam $\langle F \rangle$ and the forward- and backward-propagating distributions $\langle f^{\pm} \rangle$ are plotted. An f_2 truncation is used and all times are normalized to the scattering time $\bar{\tau}$.

term in the 90° pitch-angle diffusion term of Models 2–4, then $\epsilon \approx 0.1$ describes the wave model with resonant scattering and the upper limit of the dynamical turbulence model; $\epsilon \approx 0.01$ describes the wave model with non-resonant scattering and the lower limit of the dynamical turbulence model, and $\epsilon \approx 10^{-4}$ describes the dynamical turbulence model for mildly relativistic electrons.

Figure 11 illustrates the case of $\epsilon = 0.1$ for a rightward-propagating ring beam. The omnidirectional distribution function $\langle f \rangle$ is plotted as the solid curve, together with the various components of $\langle f \rangle$. Neither the intermediate case, $\epsilon = 0.01$, nor the very slow scattering case, $\epsilon = 10^{-4}$, is illustrated since the differences between each of the cases is very slight.

The initial beam is seen to evolve quite differently from the corresponding mirroring models. After one scattering time $t/\bar{\tau} = 1$, no perceptible differences are present, but by $t/\bar{\tau} = 5$, the rightward-propagating beam is much less pronounced than the corresponding mirroring case. The distribution at $t/\bar{\tau} = 5$ has relaxed spatially into an almost normal distribution with equal numbers of particles occupying the forward and backward hemispheres.

https://doi.org/10.1017/S0022377803002745 Published online by Cambridge University Press

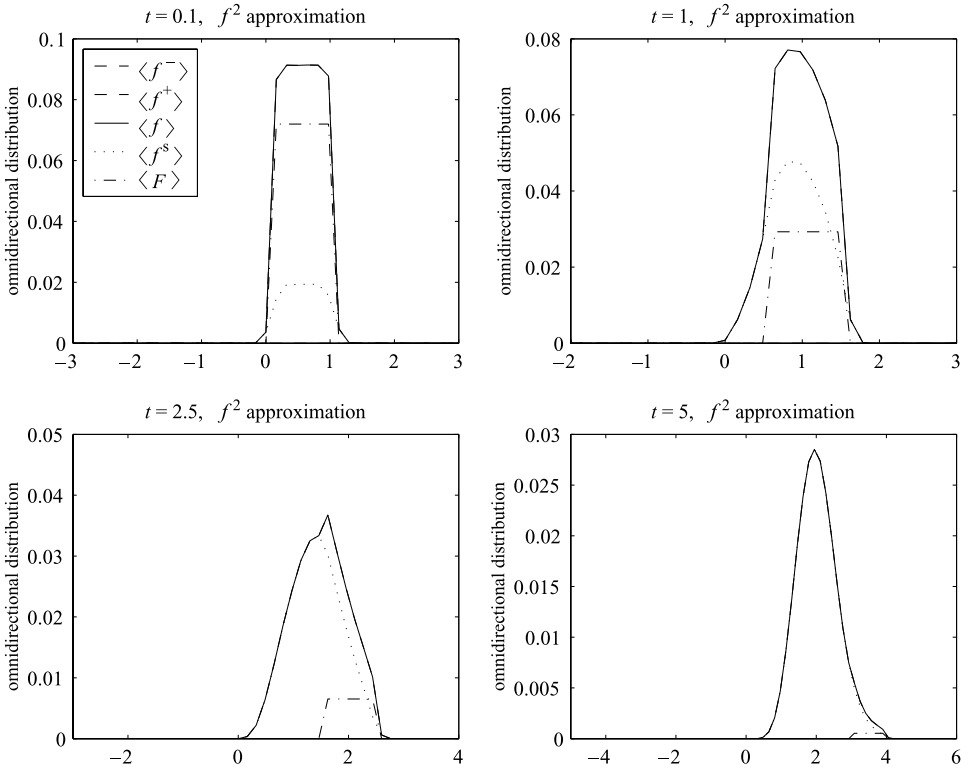

Figure 11. The temporal evolution of a right-propagating ring beam for the normalized times $t/\tau = 0.1, 1, 2.5, 5, 10, 20$ for the small-angle anisotropic QLT $q = \frac{5}{3}$ wave model appropriate to the non-resonant scattering of protons through 90° (Ragot 1999, 2000) for $\epsilon = 0.1$. The omnidirectional distribution function $\langle f \rangle$, the scattered distribution $\langle f^{s} \rangle$, the beam $\langle F \rangle$ and the forward- and backward-propagating distributions $\langle f^{\pm} \rangle$ are plotted. An f_2 truncation is used and all times are normalized to the scattering time $\bar{\tau}$.

6. Conclusions

The conclusions to emerge from this work are several and may be enumerated as follows:

(i) We have extended the propagating source method, introduced in Paper 1 to solve the Boltzmann equation with a relaxation time scattering operator, to include the quasi-linear diffusion scattering operator. Like the analysis presented in Paper 1, a half-range polynomial expansion method was used to reduce the integral-diffusion form of the 'collisional' Boltzmann equation to an infinite set of linear hyperbolic partial differential equations in the harmonics of the polynomial expansion. The lowest-order truncation of the coupled set of equations yielded an inhomogeneous form of the well-known telegrapher equation. Unlike the homogeneous telegrapher equation, which had been introduced previously to describe particle propagation in a scattering medium (Fisk and Axford 1969), the inhomogeneous form derived here and in Paper 1 does not introduce physically unrealistic pulse solutions. The form

https://doi.org/10.1017/S0022377803002745 Published online by Cambridge University Press

and coefficients of the telegrapher equation derived from the QLT model are very similar to that derived on the basis of the relaxation-time description for particle scattering. The characteristic speeds admitted by the nth order truncation of the infinite-order set of equations correspond to the 'speeds' into which the particles are scattered. As in Paper 1, even-order truncations are inherently more accurate than odd-order truncations for isotropic scattering models. In the case of anisotropic scattering, for which the half-range expansion models were introduced, it does not matter whether one uses an even- or an odd-order truncation. In either case, the propagating source method ensures that low-order truncations are very accurate.

(ii) For QLT scattering models that are not isotropic, such as when the power law index q of the power spectrum of magnetic fluctuations satisfies $q > 1$, the standard QLT pitch-angle diffusion model introduces either very slow scattering through 90° ($1 < q < 2$) or no scattering through 90° ($q \geqslant 2$). We therefore considered four augmentations to standard QLT designed to address these difficulties, namely mirroring, dynamical turbulence and two wave models.

(iii) By assuming that mirroring is responsible for scattering particles through 90° and using the standard QLT pitch-angle diffusion model to describe scattering within the forward and backward hemispheres, we investigated how solutions differed between models that use a relaxation time scattering operator and models that use a standard QLT pitch-angle diffusion model. It was found that the QLT isotropic and anisotropic models could be rather well approximated by relaxation time scattering models, at least for the reduced form of the Boltzmann equation (1.2) considered here.

(iv) As an application of our general study, we briefly considered the implications of the four models introduced to redress the difficulties faced by QLT in describing scattering through 90° (point (ii) above). In particular, for the non-mirroring models we introduced a parameter ϵ, which measured the relative rate of scattering within the hemispheres and from one hemisphere to the other. Relatively strong scattering, $\epsilon \approx 0.1$, between the hemispheres corresponds to a wave model with resonant scattering or the upper limit of the dynamical turbulence model. The intermediate case, $\epsilon \approx 0.01$, describes the wave model with non-resonant scattering or the lower limit of the dynamical turbulence model. In both cases, the propagating beam behaves quite differently from the corresponding mirroring model, with relaxation of the initial beam occurring far more rapidly for either dynamical turbulence or wave models with resonant scattering through 90° than for mirroring models. Finally, the case $\epsilon \approx 10^{-4}$ describes the dynamical turbulence model for mildly relativistic electrons. We found few discernible differences in the evolution of the distribution function between the various values of ϵ.

Acknowledgements

The partial support of NASA grants NAG5-12903 and NAG5-11621, and NSF grants ATM-0296113 and ATM-0296114 is acknowledged.

References

Bhatnager, P. L., Gross, E. P. and Krook, M. 1954 *Physical Review*, **94**, 511.

Bieber, J. W. and Matthaeus, W. H. 1991 *Proc. 22nd Int. Cosmic Ray Conf., Dublin*, Vol. 3, p. 248.

Bieber, J. W. and Matthaeus, W. H. 1992 *Particle Acceleration in Cosmic Plasmas* AIP Conference Proceedings, Vol. 264 (ed. G. P. Zank and T. K. Gaisser). New York: AIP, p. 86.

Bieber, J. W., Matthaeus, W. H., Smith, C. W., Wanner, W., Kallenrode, M.-B. and Wibberenz, G. 1994 *Astrophys. J.* **420**, 294.

Bieber, J. W., Smith, C. W. and Matthaeus, W. H. 1988 *Astrophys. J.* **334**, 470.

Davila, J. M. and Scott, J. S. 1984 *Astrophys. J.* **285**, 400.

Dröge, W. 1994 *Astrophys. J. Suppl.* **90**, 567.

Dröge, W. 2000a *Space Sci. Rev.* **93**, 121.

Dröge, W. 2000b *Astrophys. J.* **573**, 1073.

Dröge, W. and Schlickeiser, R. 1993 *Proc. 23rd Int. Cosmic Ray Conf., Calgary*, Vol. 3, p. 199.

Earl, J. A. 1995 *Proc. 24th Int. Cosmic Ray Conf.*, Vol. 4, p. 293.

Fedorov, Yu I. and Shakhov, B. A. 1993 *Proc. 23rd Int. Cosmic Ray Conf., Calgary*, Vol. 3, p. 215.

Fedorov, Yu. I., Shakhov, B. A. and Stehlik, M. 1995 *Astron. Astrophys.* **302**, 623.

Fisk, L. A. and Axford, W. I. 1969 *Sol. Phys.* **7**, 46.

Fisk, L. A., Schwadron, N. A. and Gloeckler G. 1997 *Geophys. Res. Lett.* **24**, 93.

Galeev, A. A. and Sagdeev, R. Z. 1988 *Astrophys. Space. Sci.* **144**, 427.

Glassmeier, K.-H., Coates, A. J., Acuna, M. H., Goldstein, M. L., Neubauer, F. M., Johnstone, A. D. and Réme, H. 1989 *J. Geophys. Res.* **94**, 37.

Gloeckler, G. and Geiss, J. 1998 *Space Sci. Rev.* **86**, 127.

Goldstein, M. L. 1976 *Astrophys. J.* **204**, 90.

Goldstein, M. L., Klimas, A. J. and Sandri, G. 1974 *Astrophys. J.* **195**, 787.

Gombosi, T. I., Jokipii, J. R., Kota, J., Lorencz, K. and Williams, L. L. 1993 *Astrophys. J.* **403**, 377.

Hasselmann, K. and Wibberenz, G. 1968 *Z. Geophys.* **34**, 353.

Isenberg, P. A. 1997 *J. Geophys. Res.* **102**, 4719.

Jokipii, J. R. 1966 *Astrophys. J.* **146**, 480.

Jones, F. C., Birmingham, T. J. and Kaiser, T. B. 1978 *Phys. Fluids* **21**, 347.

Kota, J. 1994 *Astrophys. J.* **427**, 1035.

Lee, M. A. and Ip, W.-H. 1987 *J. Geophys. Res.* **92**, 11 041.

le Roux, J. A., Zank, G. P., Ptuskin, V. S. and Moraal, H. 1999 *J. Geophys. Res.* **104**, 24 845.

Lu, J. Y. and Zank, G. P. 2001 *J. Geophys. Res.* **106**, 5709.

Lu, J. Y., Zank, G. P., Rankine, R. and Marchand, R. 2002 *Astrophys. J.* **576**, 574.

Lu, J. Y., Zank, G. P., Rice, W. K. M. and Webb, G. M. 2001 *Astrophys. J.* **549**, 34.

Matthaeus, W. H., Bieber, J. W. and Zank, G. P. 1995 *Rev. Geophys. Suppl.* 609.

Owens, A. J. 1974 *Astrophys. J.* **191**, 235.

Ragot, B. R. 1999 *Astrophys. J.* **518**, 974.

Ragot, B. R. 2000 *Astrophys. J.* **536**, 455.

Ruffolo, D. and Khumlumlert, T. 1995 *Geophys. Res. Lett.* **22**, 2073.

Schlickeiser, R. 1988 *J. Geophys. Res.* **93**, 2725.

Schlickeiser, R. 1989 *Astrophys. J.* **336**, 243.

Schlickeiser, R. and Achatz, U. 1993 *J. Plasma Phys.* **49**(1), 63.

Schlickeiser, R., Dung, R. and Haekel, U. 1991 *Astron. Astrophys.* **242**, L5.

Schwadron, N. A. 1998 *J. Geophys. Res.* **103**, 20 643.

Skilling, J. 1971 *Astrophys. J.* **170**, 265.

Smith, C. W. 1992 *Particle Acceleration in Cosmic Plasmas* (ed. G. Zank and T. Gaisser). American Institute of Physics Conference Proceedings, 79. New York: AIP.

Smith, C. W., Bieber, J. W. and Matthaeus, W. H. 1990 *Astrophys. J.* **363**, 283.

Webb, G. M., Zank, G. P., Pantazopoulou, M. and Zakharian, A. K. 1999 *Proc. 26th Int. Cosmic Ray Conf., Utah*, Vol. 6, p. 351.

Webb, G. M., Pantazopoulou, M. and Zank, G. P. 2000 *J. Phys. A: Math. Gen.* **33**, 3137.

Williams, L. L. and Zank, G. P. 1994 *J. Geophys. Res.* **99**, 19 229.

Völk, H. J. 1973 *Astrophys. Space Sci.* **25**, 471.

Völk, H. J. 1975 *Rev. Geophys. Space Phys.* **13**, 547.

Zank, G. P., Matthaeus, W. H., Bieber, J. W. and Moraal, H. 1998 *J. Geophys. Res.* **103**, 2085.

Zank, G. P., Lu, J. Y., Rice, W. K. M. and Webb, G. M. 1999 *Proc. 26th Int. Cosmic Ray Conf., Utah*, Vol. 6, p. 312.

Zank, G. P., Lu, J. Y., Rice, W. K. M. and Webb, G. M. 2000 *J. Plasma Phys.* **64**, 507. (Paper 1)